Collective resonances in $\chi^{(3)}$: A QED study

Konstantin E. Dorfman* and Shaul Mukamel†
Department of Chemistry, University of California, Irvine, Irvine, California 92697-2025, USA
(Received 8 February 2013; published 20 June 2013)

We calculate the third-order susceptibility $\chi^{(3)}$ of a pair of two-level atoms that interact via the exchange of photons. QED corrections to second order in coupling to vacuum field modes yield collective two-photon absorption resonances, which can be observed in transmission spectroscopy of shaped broadband pulses. While some collective effects can be obtained by introducing an effective interatomic coupling using a quantum master equation, the predicted signals contain distinct features that are missed by that level of theory and require a full diagrammatic QED treatment.

DOI: 10.1103/PhysRevA.87.063831 PACS number(s): 42.65.An, 42.50.Ct, 42.50.Hz

I. INTRODUCTION

Many-body effects strongly influence electronic and optical properties of atoms, molecules, and materials [1–5]. Collective resonances that involve several particles in multidimensional spectroscopy [6] provide clear signatures of these effects. Delocalized excitons play a key role in the function of light harvesting antennas and reaction centers [7–10]. Quantum information processing schemes [11] have been proposed that exploit collective resonances due to long-range dipole-dipole coupling [12].

In this paper we use a diagrammatic approach to calculate the transmission of a broadband pulse to fourth order in coupling to classical modes and second order in the coupling to quantum vacuum modes. Calculations are made in the joint field plus matter space [13] starting with the multipolar Hamiltonian [13–16] where all couplings are mediated by the exchange of photons. We find QED contributions to the semiclassical (SC) susceptibility $\chi^{(3)}$ that originate from mixed time ordering of interactions with vacuum and classical modes. These result in collective resonances that can be probed by shaped broadband pulses.

Shaped femtosecond pulses [17,18] have been extensively used as a tool for coherent control of the fundamental processes in various systems [19–21]. The combination of narrowband and broadband laser fields has been used in excited-state coherent anti-Stokes Raman scattering measurements [18,22–26]. We find that such pulses can suppress the background of the single-particle resonances and highlight the collective resonances. The phase profile of the broadband field relative to narrowband provides a coherent control tool for manipulating the collective resonances.

The response of a quantum system to classical optical fields is commonly described by SC susceptibilities [6]. These are calculated by sums over states of matter. Spontaneous emission is included either phenomenologically or via a quantum master equation (QME) [27,28]. The new collective resonances are induced by weak coupling to vacuum modes [29], which causes QED corrections to SC susceptibilities. The QME provides an approximate description of QED effects and can only partially account for these resonances.

*kdorfman@uci.edu
†smukamel@uci.edu

II. THE HAMILTONIAN

The multipolar Hamiltonian for two systems A and B and the radiation field is given by [13,16] $H = H_0 + H_{\rm int}$, where H_0 is the unperturbed Hamiltonian

$$H_0 = H_A + H_B + H_F \tag{1}$$

and the matter Hamiltonian reads

$$H_A + H_B = \hbar\omega_A \hat{\sigma}_A^{(z)} + \hbar\omega_B \hat{\sigma}_B^{(z)}, \tag{2}$$

with $\sigma^{(z)}$ Pauli matrices. The field Hamiltonian is

$$H_F = \frac{1}{2}\int d\mathbf{r}[\epsilon_0|\hat{\mathbf{E}}(\mathbf{r})|^2 + \mu_0|\hat{\mathbf{H}}(\mathbf{r})|^2]. \tag{3}$$

The field-matter interaction in the rotating-wave approximation written in the interaction picture with respect to H_0 is

$$H_{\rm int}(t) = \int d\mathbf{r}\,\hat{\mathbf{E}}^\dagger(t,\mathbf{r})\hat{\mathbf{V}}(t,\mathbf{r}) + \text{H.c.}, \tag{4}$$

where $\hat{\mathbf{V}}(t,\mathbf{r}) = \sum_\alpha \hat{\mathbf{V}}^\alpha(t)\delta(\mathbf{r}-\mathbf{r}_\alpha)$ is a matter operator representing the lowering (exciton annihilation) part of the dipole coupling and α run over atoms located at $\mathbf{r}_\alpha$. The field operator is

$$\hat{\mathbf{E}}(t,\mathbf{r}) = \sum_{\mathbf{k}_s,\mu}\left(\frac{2\pi\hbar\omega_s}{\Omega}\right)^{1/2}\epsilon^{(\mu)}(\mathbf{k}_s)\hat{a}_{\mathbf{k}_s}e^{-i\omega_s t + i\mathbf{k}_s\cdot\mathbf{r}}, \tag{5}$$

where $\epsilon^{(\mu)}(\mathbf{k})$ is the unit electric polarization vector of mode $(\mathbf{k}_s,\mu)$ (with μ the index of polarization), $\omega_s = c|\mathbf{k}_s|$, c is the speed of light, and Ω is the quantization volume. For classical field modes (represented by, e.g., the coherent state) we can replace the field operator by its expectation value $\mathbf{E}(t,\mathbf{r}) = \langle\psi|\hat{\mathbf{E}}(t,\mathbf{r})|\psi\rangle$, where ψ represents the state of light. Otherwise we treat it as an operator. We shall make use of the commutation relations [13]

$$[E^{(l)}(\tau_i,\mathbf{r}_\beta), E^{(m)\dagger}(\tau_j,\mathbf{r}_\alpha)] = \int\frac{d\omega}{2\pi}\mathcal{D}^{(l,m)}_{\alpha\beta}(\omega)e^{i\omega(\tau_j-\tau_i)}, \tag{6}$$

$$[E^{(l)}(\omega_i,\mathbf{r}_\beta), E^{(m)\dagger}(\omega_j,\mathbf{r}_\alpha)] = \mathcal{D}^{(l,m)}_{\alpha\beta}(\omega_i)\delta(\omega_i-\omega_j), \tag{7}$$

where l and m denote Cartesian components of the electric field, the coupling tensor reads [13,30]

$$\mathcal{D}^{(l,m)}_{\alpha\beta}(\omega) = \frac{\hbar}{2\pi\epsilon_0}(-\nabla^2\delta_{lm} + \boldsymbol{\nabla}_l\cdot\boldsymbol{\nabla}_m)\frac{\sin(\omega r_{\alpha\beta}/c)}{r_{\alpha\beta}}, \tag{8}$$

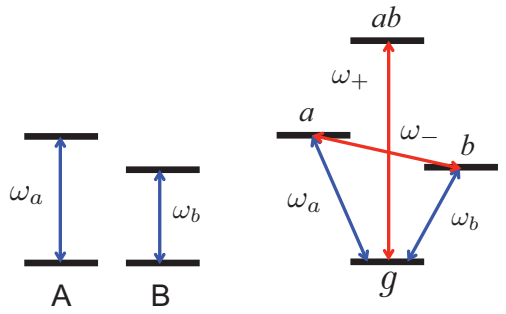

FIG. 1. (Color online) Two noninteracting atoms A and B (left) and corresponding two-particle eigenstates (right). Blue arrows represent single-particle resonances with an individual atom and red arrows correspond to a collective two-particle resonance with frequencies ω_+ (sum frequency) and ω_- (difference frequency).

and $r_{\alpha\beta} = |\mathbf{r}_\alpha - \mathbf{r}_\beta|$ is the interatomic distance. The diagonal elements $\mathcal{D}^{(l,m)}_{\alpha\alpha}(\omega) = \hbar\omega^3/2\pi\epsilon_0 c^3\delta_{lm}$ represent the self-energy corrections, i.e., energy shifts and the cooperative emission rate, whereas the off-diagonal contribution (8) yields the cross relaxation and dipole-dipole coupling.

When classical light interacts with an ensemble of noninteracting atoms A and B, the response is additive and is given by $S(\omega) = S_A(\omega) + S_B(\omega)$, where S_A and S_B are the individual responses of each atom. For weakly coupled atoms the response acquires nonadditive terms $S_{AB}(\omega)$, which arise from interactions between atoms

$$S(\omega) = S_A(\omega) + S_B(\omega) + S_{AB}(\omega). \tag{9}$$

We shall calculate these nonadditive contributions perturbatively in light-matter interactions using QED and show that they contain two types of collective resonances: two-photon absorption (TPA) $\omega + \omega_1 = \omega_a + \omega_b$ and Raman type $\omega - \omega_1 = \omega_a - \omega_b$, where ω and ω_1 are two field modes of the transmitted pulse and ω_a and ω_b are transition frequencies of the two atoms A and B, respectively (see Fig. 1). We show that the signal may not be fully described by an effective Hamiltonian alone, but a complete QED treatment is needed. We further show how such resonances may be observed and distinguished from noncollective single-particle resonances.

III. TRANSMISSION OF A BROADBAND PULSE TO SECOND ORDER IN COUPLING TO VACUUM MODES

We assume that the system interacts with a classical broadband shaped pulse $E(\omega,\mathbf{r}) = \int_{-\infty}^{\infty} dt\, E(t) e^{i\omega t - i\mathbf{k}_0\cdot\mathbf{r}}$, where we assume that all frequency components of the incoming pulse have the same wave vector $\mathbf{k}_0$ (paraxial approximation). We focus on the frequency-dispersed transmission

$$S(\omega) = \frac{2}{\hbar}\int_{-\infty}^{\infty} d\mathbf{r}\, \mathrm{Im}[E^*(\omega,\mathbf{r})P(\omega,\mathbf{r})], \tag{10}$$

where Im denotes the imaginary part and

$$P(\omega,\mathbf{r}) = \int_{-\infty}^{\infty} dt\, P(t,\mathbf{r}) e^{i\omega t} \tag{11}$$

is the Fourier transform of the polarization. We shall calculate P perturbatively in the field-matter interaction [Eq. (4)]. To maintain a convenient bookkeeping of time-ordered Green's functions we adopt superoperator notation. With every ordinary operator O we associate two superoperators defined by their action on an ordinary operator X as $O_L = OX$ acting from the left and $O_R = XO$ from the right. We further define the symmetric and antisymmetric combinations $O_+ = \frac{1}{2}(O_L + O_R)$ and $O_- = O_L - O_R$. Without loss of generality we assume that the last interaction results in deexcitation of the matter with consequent emission of the photon and express the nonlinear polarization using superoperators in the interaction picture

$$P(t,\mathbf{r}) = \left\langle \mathcal{T} V_L(t,\mathbf{r}) \exp\left(-\frac{i}{\hbar}\int_{-\infty}^{t} H_-(\tau)d\tau\right)\right\rangle, \tag{12}$$

where $\langle\cdots\rangle = \mathrm{Tr}[\rho_0\cdots]$ is understood with ρ_0 the initial field plus matter density operator and $\mathcal{T}$ the time-ordering operator.

The linear response is obtained by calculating the signal to second order in the coupling to the classical field. QED corrections to the linear response are obtained to fourth order in field-matter interactions (two with the classical modes and two with vacuum modes). The transmitted classical field scales as $\sim|E(\omega)|^2$, which contributes to the linear response. The latter correction to the linear response is phase independent and cannot be manipulated by coherent control schemes. The lowest-order contribution to the nonlinear response that contains phase information of the incoming pulse and has nonadditive contributions that may reveal collective resonances involves six field-matter interactions (four with a classical broadband pulse and two with quantum vacuum modes that mediate the interaction between atoms).

We assume that the system is initially in the ground state g. The relevant diagrams responsible for collective effects when the last emission occurs from atom A are shown in Fig. 2. Similar set of diagrams can be obtained when the last emission is from atom B. The total signal is given by the sum of the pathways corresponding to each diagram, $S_A(\omega) = \sum_i S_{Ai}(\omega)$, and can be read off the diagrams of Fig. 2 (see Appendix A).

The classical response function is given by the diagrams in Fig. 2. These result in Eqs. (A1)–(A14), which use normally ordered field operators. The field correlation function of normally ordered operators when the field is in a coherent state, which is the closest to the classical, may be factorized into a product of field amplitudes. Terms where the field operators are not normally ordered exist in several pathways. They can be brought into a normally ordered form by making use of the commutation relations (6) and (7). These apply to the quantum modes of the radiation field (wavy lines in Fig. 2) that are initially in a vacuum state.

The total signal including the diagrams where the last emission is with atom B is

$$\begin{aligned} S(\omega) = \mathrm{Im}\frac{NAB|\mu_a|^2|\mu_b|^2}{2\pi\hbar^6}\int_{-\infty}^{\infty}\frac{d\omega_1}{2\pi}\frac{d\omega_2}{2\pi} \\ \times E^*(\omega)E^*(\omega_1)E(\omega+\omega_1-\omega_2)E(\omega_2) \\ \times \chi^{(3)}_{QED}(-\omega,-\omega_1,\omega+\omega_1-\omega_2,\omega_2), \end{aligned} \tag{13}$$

where N denotes the number of A-B pairs. For reasons that will become clear later, we partition $\chi^{(3)}_{QED}$ into two groups of terms $\chi^{(3)}_{QED} = \chi^{(3)}_I + \chi^{(3)}_{II}$. Both can be read from the diagrams

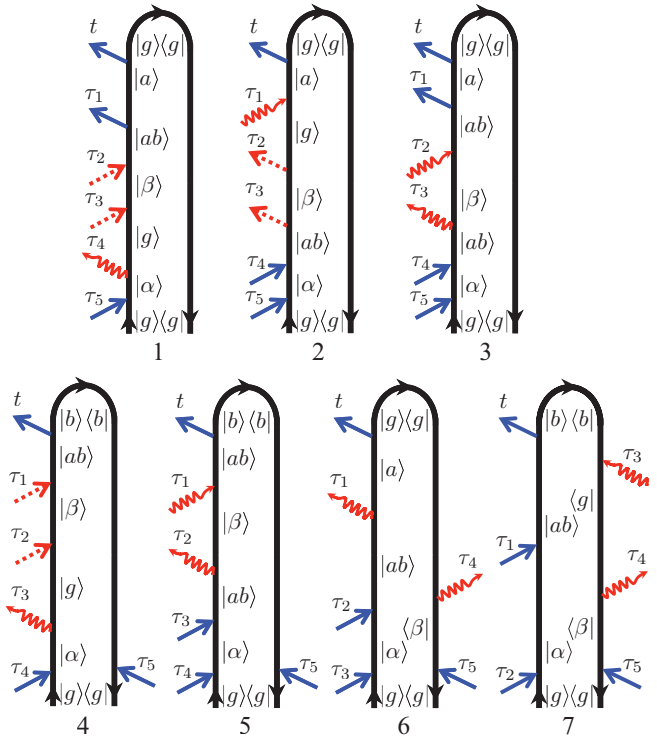

FIG. 2. (Color online) Loop diagrams (for rules see [31]) for the frequency-dispersed transmission signal (10) from a pair of noninteracting atoms A and B, $\alpha,\beta = a,b$, that are initially prepared in the ground state g generated by four interactions with classical light and two with quantum field modes. Shown are diagrams where the last interaction is with atom A. Interchanging A and B will yield another set of diagrams. Straight blue arrows represent the field-matter interaction of classical light with atoms. Wavy red lines correspond to quantum modes and dashed red lines represent interactions with both classical and quantum modes.

in Fig. 2 and are given in Appendix A:

$$\chi^{(3)I} = \sum_{j=1}^{3} \chi^{(3)I}_{jLLLL}(-\omega,-\omega_1,\omega+\omega_1-\omega_2,\omega_2) + \sum_{j=4,5,7} \left[\chi^{(3)I}_{jLLLR}(-\omega,-\omega_1,\omega+\omega_1-\omega_2,\omega_2) + \chi^{(3)I}_{jL\leftrightarrow R}\right], \tag{14}$$

$$\chi^{(3)II} = \int \frac{d\omega'}{2\pi}\Big[\chi^{(5)II}_{1LLLLLL}(-\omega,-\omega_1,\omega',\omega+\omega_1-\omega_2,-\omega',\omega_2) + \chi^{(5)II}_{2LLLLLL}(-\omega,\omega',-\omega_1,-\omega',\omega+\omega_1-\omega_2,\omega_2) + \chi^{(5)II}_{4LLLLLR}(-\omega,-\omega_1,\omega',\omega+\omega_1-\omega_2,-\omega',\omega_2) + \chi^{(5)II}_{4L\leftrightarrow R} + \chi^{(5)II}_{6LLLLRR} \times(-\omega,\omega',-\omega_1,-\omega',\omega+\omega_1-\omega_2,\omega_2) + \chi^{(5)II}_{6L\leftrightarrow R}\Big], \tag{15}$$

where the numerical subscript corresponds to the diagrams in Fig. 2 and various permutations of left and right interactions for diagrams 4 and 6 are included. It follows from the expressions given in Appendix A that $\chi^{(3)}_{QED}$ contains a TPA collective resonance that contains the Green's function $G^{(+)}_{ab}(\omega+\omega_1) = i/[\omega+\omega_1-\omega_+ + i\gamma_{ab}]$ with $\omega_+ = \omega_a+\omega_b$ and $\gamma_{ab} = \gamma_a + \gamma_b$. Here γ_α^{-1} ($\alpha = a,b$) represents the lifetime of state α that is ultimately related to the coupling constant (27) obtained from the QME treatment: $\gamma_\alpha = \mathcal{L}_{\alpha\alpha}(\omega)$ [27]. The collective resonances $\omega+\omega_1 = \omega_+ + i\gamma_{ab}$ generally washed out by the ω_1 integration. However, we shall demonstrate how these TPA resonances as well as collective Raman resonances can be recovered by pulse shaping.

IV. DETECTING COLLECTIVE RESONANCES BY SPECTROSCOPY WITH SHAPED PULSES

We assume an incoming classical pulse consisting of a long (picosecond) and broadband (femtosecond) pulses (see Fig. 3). The electric field reads

$$E(\omega) = 2\pi\mathcal{E}_1 e^{i\xi}\delta(\omega-\omega_p) + 2\pi\mathcal{E}_2 e^{i\phi(\omega)}. \tag{16}$$

We shall use the amplitudes $\mathcal{E}_1$ and $\mathcal{E}_2$ and the phases ξ and $\phi(\omega)$ of these two fields as control parameters. The signal (13) depends on the product of field amplitudes

$$\begin{aligned}&\frac{1}{(2\pi)^2}E^*(\omega)E^*(\omega_1)E(\omega+\omega_1-\omega_2)E(\omega_2)\\ &= \mathcal{E}_2^2\mathcal{E}_1^2\{\delta(\omega_1-\omega_p)[\delta(\omega_2-\omega)+\delta(\omega_2-\omega_p)]\\ &\quad + \delta(\omega+\omega_1-2\omega_p)\delta(\omega_2-\omega)e^{i[2\xi-\phi(\omega)-\phi(\omega_1)]}\}\\ &\quad + \mathcal{E}_2^3\mathcal{E}_1\{\delta(\omega_1-\omega_p)e^{i[\phi(\omega+\omega_p-\omega_2)+\phi(\omega_2)-\phi(\omega)-\xi]}\\ &\quad + \delta(\omega_2-\omega_p)e^{i[\phi(\omega+\omega_1-\omega_p)+\xi-\phi(\omega)-\phi(\omega_1)]}\\ &\quad + \delta(\omega+\omega_1-\omega_2-\omega_p)e^{i[\phi(\omega+\omega_1-\omega_p)+\xi-\phi(\omega)-\phi(\omega_1)]}\},\end{aligned} \tag{17}$$

where the last interaction that results in the last emission occurs with a broadband field $\mathcal{E}_2$ and we neglect the term $\sim\mathcal{E}_2^4$, which contains no collective resonances in (13). We shall show that the terms $\sim\mathcal{E}_2^3\mathcal{E}_1$ contain interesting phase information.

We hold the amplitude and the phase of the narrowband pulse fixed and calculate the transmission of the broadband pulse while varying its parameters. Contour integration is used to evaluate the frequency integrations in (13). We shall expand the phase $\phi(\omega)$ in a Taylor series in the vicinity of a reference frequency ω_0,

$$\phi(\omega,\{C_n\}) = \sum_n C_n\cdot(\omega-\omega_0)^n. \tag{18}$$

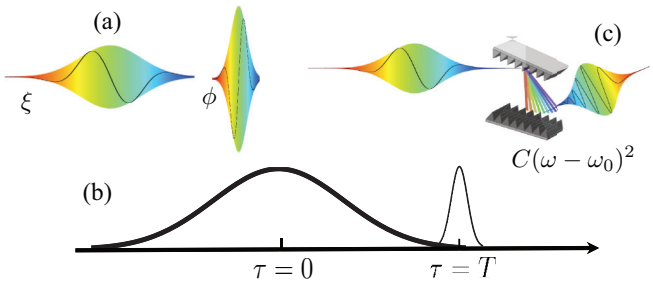

FIG. 3. (Color online) Pulse shaping for narrowband (picosecond) pulse with phase ξ and broadband (femtosecond) pulse with phase $\phi(\omega)$: (a) constant phase ϕ, (b) linear phase [time delay $\phi(\omega) = \omega T$], and (c) quadratic phase [linearly chirped $\phi(\omega) = C(\omega-\omega_0)^2$].

Here C_0, C_1, and C_2 represent a constant phase, pulse delay, and chirping, respectively. The sign of C_n defines the direction of the contour in the complex plane for evaluation of the residues in the frequency integrations. Assuming a short delay or small chirp rate, the signal (13) becomes

$$S(\omega,\omega_p) = S_I(\omega,\omega_p) + S_{II}(\omega,\omega_p), \tag{19}$$

$$S_I(\omega,\omega_p) = \mathcal{I}\frac{iN|\mu_a|^2|\mu_b|^2}{\hbar^6}\Big[\mathcal{E}_2^3\mathcal{E}_1\Big(G_{ab}^{(+)}(\omega+\omega_p)A_1(\omega,\omega_p) + G_{ab}^{(+)2}(\omega+\omega_p)A_2(\omega,\omega_p) + \sum_{\alpha,\beta,\delta}\big[G_{\beta\alpha}^{(-)}(\omega-\omega_p)A_3^{(\alpha)}(\omega,\omega_p) + G_{\beta\alpha}^{(-)}(\omega-\omega_p)G_{\delta\alpha}^{(-)}(\omega-\omega_p)A_4^{(\alpha\beta\delta)}(\omega,\omega_p) + G_{\beta\alpha}^{(-)\dagger}(\omega_p-\omega)G_{\delta\alpha}^{(-)\dagger}(\omega_p-\omega)A_5^{(\alpha\beta\delta)}(\omega,\omega_p)\big]\Big) + \mathcal{E}_2^2\mathcal{E}_1^2\big[G_{ab}^{(+)}(\omega+\omega_p)A_6(\omega,\omega_p) + G_{ab}^{(+)}(2\omega_p)A_7(\omega,\omega_p) + G_{ab}^{(+)2}(\omega+\omega_p)A_8(\omega,\omega_p) + G_{ab}^{(+)2}(2\omega_p)A_9(\omega,\omega_p)\big]\Big], \tag{20}$$

$$S_{II}(\omega,\omega_p) = \mathcal{I}\frac{iN_{AB}|\mu_a|^2|\mu_b|^2}{\hbar^6}\Big\{\mathcal{E}_2^3\mathcal{E}_1\Big(G_{ab}^{(+)}(\omega+\omega_p)B_1(\omega,\omega_p) + G_{ab}^{(+)}(\omega+\omega_p)\Big[G_{ab}^{(+)}(\omega+\omega_p)B_2(\omega,\omega_p) + G_{aa}^{(+)}(\omega+\omega_p)B_3(\omega,\omega_p) + G_{bb}^{(+)}(\omega+\omega_p)B_4(\omega,\omega_p)\Big] + \sum_{\alpha,\beta}\big[G_{\beta\alpha}^{(-)}(\omega-\omega_p)B_5^{(\alpha\beta)}(\omega,\omega_p) + G_{\beta\alpha}^{(-)}(\omega_p-\omega)B_6^{(\alpha\beta)}(\omega,\omega_p) + G_{\beta\alpha}^{(-)\dagger}(\omega_p-\omega)B_7^{(\alpha\beta)}(\omega,\omega_p)\big]\Big) + \mathcal{E}_2^2\mathcal{E}_1^2\big[G_{ab}^{(+)}(\omega+\omega_p)B_8(\omega,\omega_p) + G_{ab}^{(+)}(2\omega_p)B_9(\omega,\omega_p)\big]\Big\}. \tag{21}$$

The parameters $A_1,\ldots,A_9$ and $B_1,\ldots,B_9$ are listed in Appendix B. Here the collective Raman Green's function $G_{\alpha\beta}^{(-)}(\omega) = i/[\omega-\omega_{\alpha\beta-}+i\gamma_{\alpha\beta}]$ and the collective TPA Green's function $G_{\alpha\beta}^{(+)}(\omega) = i/[\omega-\omega_{\alpha\beta+}+i\gamma_{\alpha\beta}]$ with $\omega_{\alpha\beta\pm} = \omega_\alpha \pm \omega_\beta$, $\gamma_{\alpha\beta} = \gamma_\alpha + \gamma_\beta$, and $\alpha,\beta = a,b$.

The signals (20) and (21) contain the TPA Green's function $G_{ab}^{(+)}$ as well as Raman-type collective resonances governed by the Green's function $G_{\beta\alpha}^{(-)}$. The latter are of two types: $\alpha=\beta$ elastic (Rayleigh) scattering and $\alpha\neq\beta$ Raman. The Rayleigh resonance contains a factor of 2 compared to the Raman contribution due to permutations for $\alpha\leftrightarrow\beta$. This causes N^2 vs N scaling of the signal, respectively.

The narrowband and broadband field amplitudes allow for additional control over the resonance features. If the broadband pulse is strong, the signal (20) generated by an A-B pair of different atoms shows only one type of TPA resonance $\omega+\omega_p=\omega_a+\omega_b$, whereas (21) has two additional additional types $\omega+\omega_p=2\omega_a$ and $2\omega_b$ (see Appendix B). The latter resonances are missing if multiple interactions occur within the single atom and therefore constitute a collective nature. Clearly, these types of resonances will appear in the signal (20) for a pair of atoms of the same type, A-A or B-B. However, in an arbitrary sample composed of several species depending on the density of the sample as well as the dipole moments μ_a vs μ_b it is possible to obtain the couplings between atoms of different types. In certain parameter regimes, for example, for a gas of two types of atoms, signals S_I and S_{II} predict different resonances.

V. SIMULATIONS

We now compare the relative strength of the collective resonances and show how they can be controlled by the nonlinear phase $\phi(\omega)$. Consider a system of two atoms A and B with transition frequencies $\omega_a = 13\,000$ cm^{-1} and $\omega_b = 11\,000$ cm^{-1} and linewidth $\gamma_a=\gamma_b=200$ cm^{-1}. In Fig. 4 we depict the signal $S(\omega,\omega_p)$ vs the broadband frequency ω for a fixed off-resonant $\omega_p = 4000$ cm^{-1} and $\mu_B \simeq 0.99\mu_A$. In this section we discuss only the full signal given by Eq. (19) (red solid line). The S_I contribution from Eq. (20) (black dashed line) will be discussed in Sec. VI.

It is apparent that only $\mathcal{E}_2^3\mathcal{E}_1$ terms in Eqs. (20) and (21) contain a Raman-type resonance, whereas the $\mathcal{E}_2^2\mathcal{E}_1^2$ terms yield TPA resonances. The TPA resonance is weaker than the Raman and single-photon resonances in most of the parameter regimes. One can probe the $\mathcal{E}_2^3\mathcal{E}_1$ and $\mathcal{E}_2^2\mathcal{E}_1^2$ terms separately due to the different intensity dependence.

In the following simulations we focus on the $\mathcal{E}_2^3\mathcal{E}_1$ that contain both Raman and TPA collective resonances. We consider three models for the phase $\phi(\omega)$: (i) a constant phase $\phi(\omega)=\xi+\Delta\phi$, (ii) a linear phase [32] $\phi(\omega)=\omega T$ that induces a delay T of the broadband pulse relative to the narrowband, and (iii) a quadratic phase $\phi(\omega)=C_2(\omega-\omega_0)^2$ that represents linear chirp [33] with reference frequency $\omega_0=(\omega_a+\omega_b)/2$.

We start with model (i). Figure 4(a) shows that for a fixed off-resonant narrowband frequency $\omega_p = 4000$ cm^{-1} the spectra has two Raman $\omega=2000$ and 6000 peaks and one Rayleigh peak $\omega\sim 4000$ cm^{-1}, two single-photon

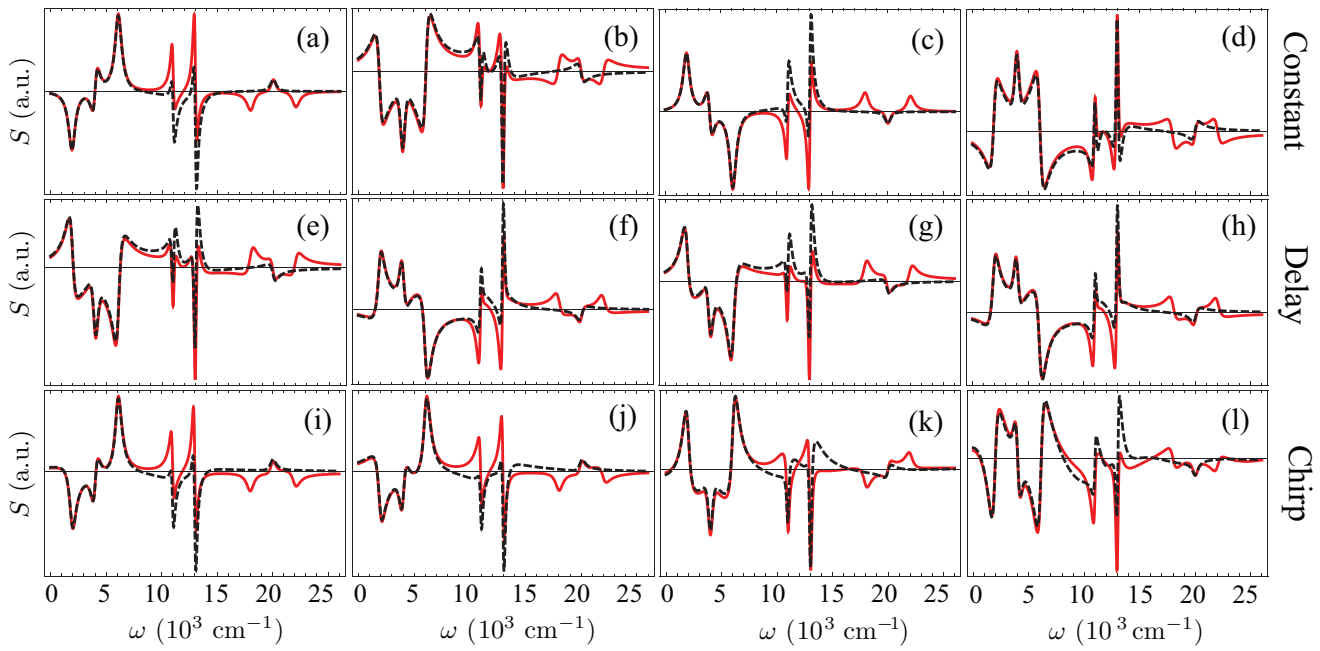

FIG. 4. (Color online) The top row shows the frequency-dispersed transmission signal for pairs of atoms. The constant phases are (a) $\Delta\phi = 0$, (b) $\Delta\phi = \pi/2$, (c) $\Delta\phi = \pi$, and (d) $\Delta\phi = 3\pi/2$. The red solid line gives the full signal (19). The black dashed line represents Eq. (20). The middle row shows the variable delay T for (e) 17 fs, (f) 33 fs, (g) 330 fs, and (h) 3.3 ps. The bottom row shows the linear chirp C_2 equal to (i) 5×10^{-9} cm^{-2}, (j) 10^{-8} cm^{-2}, (k) 2.5×10^{-8} cm^{-2}, and (l) 5×10^{-8} cm^{-2}.

resonances at $\omega = \omega_a$ and ω_b, and a two-photon resonance $\omega = \omega_a + \omega_b - \omega_p \sim 20\,000$ cm^{-1}. The signal (19) contains two additional TPA peaks at $\omega = 2\omega_a - \omega_p = 22\,000$ cm^{-1} and $\omega = 2\omega_b - \omega_p = 18\,000$ cm^{-1}. We next turn to the TPA resonances. If $\Delta\phi_0 = 0,\pi$ Figs. 4(a) and 4(c) peak at $\omega_a + \omega_b$, which corresponds to emission, and have a dip at $2\omega_a$ and $2\omega_b$, corresponding to absorption. For $\Delta\phi_0 = \pi/2,3\pi/2$ [Figs. 4(b) and 4(d)] the situation is different. It corresponds to a destructive quantum interference of absorption and emission pathways corresponding to two atoms (e.g., Fano interference) and all three TPA peaks become asymmetric.

Model (ii) is shown in Figs. 4(e)–4(h). The interplay between destructive interference (asymmetric), absorption (dip), and emission (peak) for the TPA resonances is less susceptible to the delay than model (i) for the phase shift. All three TPA peaks show quantum interference for the entire range of delays from 17 fs to 3.3 ps shown in Figs. 4(e)–4(h).

The resonance pattern for model (iii) is more complex. For small positive chirp rate $C_2 = 5 \times 10^{-9}$–10^{-8} cm^{-2} [Figs. 4(i) and 4(j)] all three TPA peaks are symmetric, where $2\omega_a$ and $2\omega_b$ correspond to absorption (dip) and $\omega_a + \omega_b$ has a peak (emission). For moderate chirp rate $C_2 = 2.5 \times 10^{-8}$ cm^{-2} [Fig. 4(k)] the $\omega_a + \omega_b$ peak becomes asymmetric, which corresponds to the regime of destructive interference, and two symmetric peaks at $2\omega_a$ and $2\omega_b$ now have different sign, corresponding to emission (peak) for one and absorption (dip) for the other. For larger chirp rate $C_2 = 5 \times 10^{-8}$ cm^{-2} [Fig. 4(k)] the collective resonances are slightly less pronounced compared to the single-photon peaks, whereas for negative chirp $C_2 = -5 \times 10^{-8}$ cm^{-2} [Fig. 4(l)] the situation becomes the opposite: Two peaks $2\omega_a$ and $2\omega_b$ are asymmetric (interference) and $\omega_a + \omega_b$ corresponds to absorption (dip).

To better distinguish between various collective and single photon resonances we display a two-dimensional signal vs the broadband ω and the narrowband ω_p frequencies. Chirping [model (iii)] allows us to eliminate the background by looking at the residue signal shown in Fig. 5 defined as the difference of two measurements with opposite sign of chirp

$$S_r(\omega,\omega_p) \equiv S(\omega,\omega_p,C_2) - S(\omega,\omega_p,-C_2). \qquad (22)$$

Figure 5(a) shows the A-B system. It contains two types of single-photon resonances shown by vertical lines due to single-photon resonance with the broadband field at $\omega = \omega_a$ and ω_b and 45° inclined lines corresponding to the single-photon resonance with the narrowband field at $\omega_p = \omega_a$ and ω_b. In addition, we observe three collective TPA peaks depicted by horizontal lines at $\omega + \omega_p = \omega_a + \omega_b = 24\,000$ cm^{-1}, $\omega + \omega_p = 2\omega_a = 26\,000$ cm^{-1}, and $\omega + \omega_p = 2\omega_b = 22\,000$ cm^{-1} as predicted by Eq. (19). For the A-A and B-B systems shown in Figs. 5(b) and 5(c), respectively, the corresponding collective resonance is given by a single TPA resonance at $\omega + \omega_p = 2\omega_a$ and $\omega + \omega_p = 2\omega_b$, respectively.

Calculation using partial signal (20) results in a single TPA resonance for all three types of system: $\omega_\alpha + \omega_\beta$ for $\alpha + \beta$, $\alpha,\beta = A,B$, which is illustrated in Figs. 5(d)–5(f). The latter arises from diagram 4 in Fig. 2 and corresponds to the following situation. Initial excitation by the incoming pulse that acts on both bra and ket brings the system to the nonstationary density matrix, which then radiates a spontaneous photon leaving the system in the excited- to ground-state coherence. After the second interaction with incoming pulse, which promotes the system to a single excited state, the spontaneous photon emitted by the first atom is finally absorbed by the second atom, which forces the two-atom system to the double- to single-excited-state coherence. It

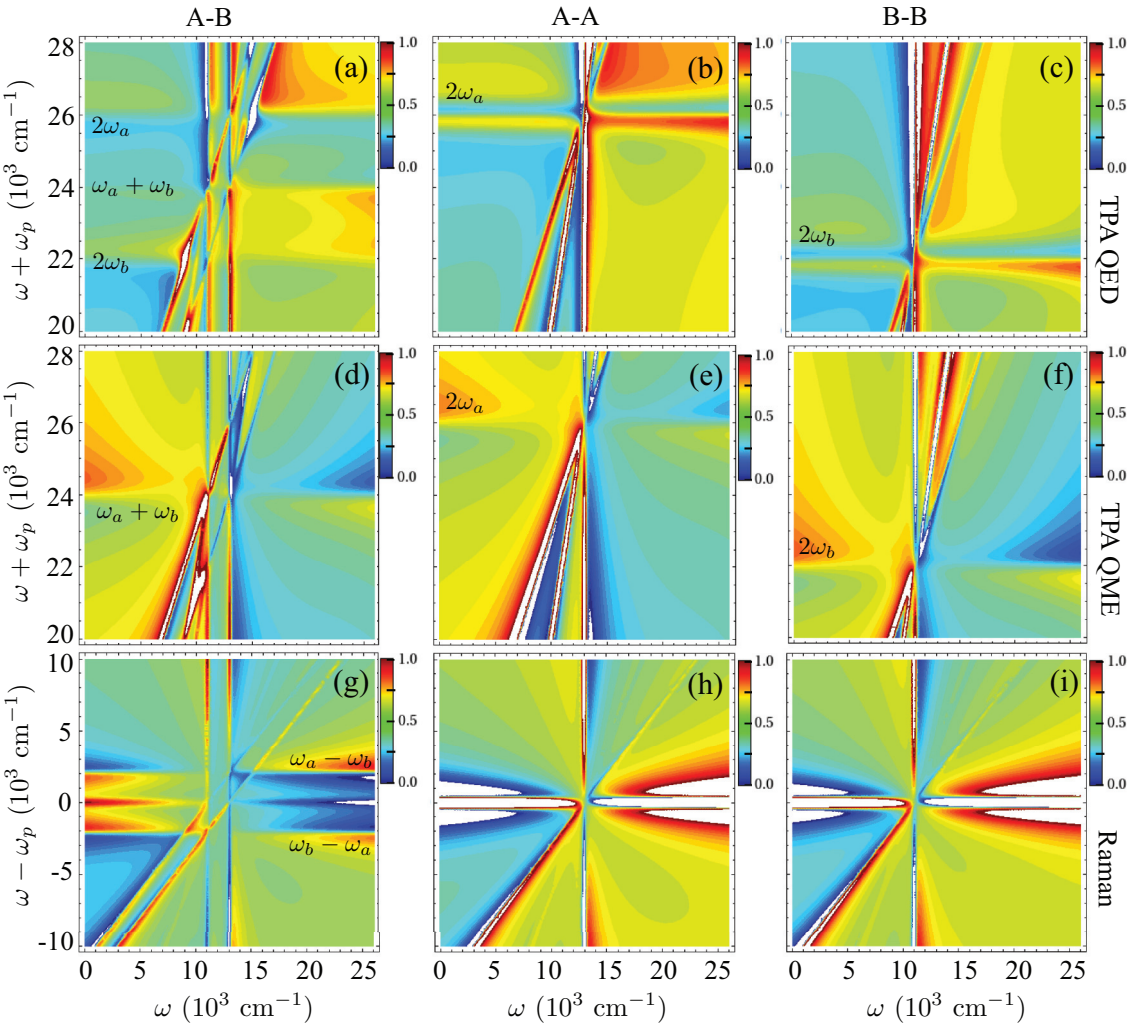

FIG. 5. (Color online) Frequency-dispersed residue signal (22) with linear chirped broadband pulse with chirp rate $C_2 = 5 \times 10^{-9}$ cm^{-2}: left column, the A-B system; middle column, the A-A system; right column, the B-B system; top row, result of Eq. (19); middle row, result of Eq. (20) corresponding to TPA resonances via $S_r(\omega + \omega_p, \omega)$; bottom row, Raman resonances via $S_r(\omega - \omega_p, \omega)$ using full signal (19).

then undergoes a stimulated emission via the interaction with the incoming pulse for the fourth time and the system ends up in the single-excited-state population state. In the following we will mostly focus on TPA-type collective resonances.

The bottom row of Fig. 5 shows collective Raman resonances accessible by a signal (19). Figure 5(g) for the A-B signal contains an elastic (Rayleigh) resonance at $\omega = \omega_p$ and two Raman resonances $\omega - \omega_p = \pm\omega_a \mp \omega_b$. The A-A and B-B signals show only a Rayleigh peak [the side peaks appear due to oscillation of the nonlinear phase in the residue signal (22)].

VI. COLLECTIVE RESONANCES PREDICTED BY THE QME

The SC approach describes the coupling mediated by exchange of photons by a QME for the matter density operator

$$\dot{\rho} = -i\sum_{\alpha}\left[\omega_{\alpha}^{(0)}\sigma_{\alpha}^{(z)},\rho\right] - i\sum_{\alpha\neq\beta}\mathcal{L}_{\alpha\beta}[V_{\alpha}^{\dagger}V_{\beta},\rho] - \sum_{\alpha,\beta}\gamma_{\alpha\beta}(V_{\alpha}^{\dagger}V_{\beta}\rho - 2V_{\beta}\rho V_{\alpha}^{\dagger} + \rho V_{\alpha}^{\dagger}V_{\beta}) - i\left[H_{\rm int}^{(c)},\rho\right], \tag{23}$$

where $H_{\rm int}^{(c)}$ is the interaction Hamiltonian between matter and classical field modes, $\omega_{\alpha}^{(0)}$ is the renormalized transition frequency, $\mathcal{L}_{\alpha\beta}$ is the dipole-dipole interaction due to interaction with the common quantum mode, and $\gamma_{\alpha\beta}$ is a cooperative emission rate. The last term represents the interaction with classical field modes.

Some quantum pathways for the signal (10) can be obtained directly from the QME (23) as can be deduced from the corresponding diagrams shown in Fig. 2. If two consecutive interactions occur with quantum modes, then the signal can be obtained in the lower-order $\chi^{(3)}$ theory rather than $\chi^{(5)}$ by introducing effective interatomic couplings that originate from emission and reabsorption of the photon by a single excited state of the system through the ground state (diagrams 1, 2, 4, and 7 in Fig. 2)

$$\mathcal{L}_{\alpha\beta}(\omega) = \frac{1}{\hbar^2}\int_{-\infty}^{\infty}\frac{d\omega'}{2\pi}\mu_{\alpha}^{(l)*}\mu_{\beta}^{(m)}\mathcal{D}_{\alpha\beta}^{(l,m)}(\omega')G_g(\omega-\omega'), \tag{24}$$

where summation is assumed for repeating indices. Similar two-photon coupling for emission and reabsorption by a two-photon state of the system through a single-photon state

(diagrams 3 and 5 in Fig. 2) gives

$$\mathcal{L}_s(\omega+\omega_1)=\frac{1}{\hbar^2}\sum_\alpha\int_{-\infty}^{\infty}\frac{d\omega'}{2\pi}\mathcal{L}_{\alpha\alpha}(\omega')G_{\bar{\alpha}}(\omega+\omega_1-\omega'), \tag{25}$$

where $G_\alpha=i/(\omega-\omega_\alpha+i\gamma_\alpha)$ and $\bar{\alpha}=a$ if $\alpha=b$ and $\bar{\alpha}=b$ if $\alpha=a$.

Equations (24) and (25) reveal that diagrams 3, 5, and 7 of Fig. 2 can be recast via master equation (23). This is not the case for diagram 6, since two interactions with quantum modes have an additional interaction with a classical field in between. Using the same reasoning one can show that the remaining diagrams 1, 2, and 4 have both types of contributions: ones that can be recast as an effective couplings and ones that cannot. Thus $\chi_I^{(3)}$ in Eq. (14) represents the QME contribution, whereas $\chi_{II}^{(3)}$ in Eq. (15) requires the full QED description.

To explain the limitations of the QME approach we first note that the signal strongly depends on the interatomic distance. We combine the density of radiation modes (8) and coupling in Eq. (24) using an identity [13]

$$(-\nabla^2\delta_{\mu\nu}+\nabla_\mu\cdot\nabla_\nu)\frac{e^{ikR}}{R}=\frac{1}{R^3}[(\delta_{\mu\nu}-3\hat{R}_\mu\hat{R}_\nu)(ikR-1)+(\delta_{\mu\nu}-\hat{R}_\mu\hat{R}_\nu)k^2R^2]e^{ikR}. \tag{26}$$

Assuming randomly orientated atoms $\hat{R}_\mu\hat{R}_\nu=\frac{1}{3}\delta_{\mu\nu}$, we obtain a dependence on the distance $1/r_{\alpha\beta}$. Furthermore, Eqs. (20) and (21) contain coefficients A_j and B_j ($j=1,\ldots,9$) that depend on the distance between atoms via two types of couplings (see Appendix B). The coupling (24) that gives the cooperative decay rate [27]

$$\mathcal{L}_{\alpha\beta}(\omega)=\frac{\mu_\alpha^*\mu_\beta\omega^2}{3\pi\hbar\epsilon_0c^2r_{\alpha\beta}}\sin[\omega r_{\alpha\beta}/c],\quad \mathcal{L}_{\alpha\alpha}(\omega)=\frac{|\mu_\alpha|^2\omega^3}{3\pi\hbar\epsilon_0c^3}. \tag{27}$$

This rate is typically small compared to the transition frequencies (weak-coupling regime) $\mathcal{L}_{\alpha\beta}\ll\omega_\alpha$ and is finite at small distances due to the $\sin(x/x)$ factor. It enters the coefficients for most single-photon resonances and some collective Raman resonances. In addition, there is a complex coupling (see Appendix B)

$$\mathcal{M}_{\alpha\beta}(\omega)=\frac{\mu_\alpha^*\mu_\beta\omega^2}{6\pi\hbar\epsilon_0c^2r_{\alpha\beta}}[i\cos(\omega r_{\alpha\beta}/c)+\sin(\omega r_{\alpha\beta}/c)], \tag{28}$$

where the first term corresponds to a dipole-dipole interaction and the second term is half of the cooperative spontaneous emission (superradiance) rate (27). Note that the dipole-dipole coupling grows rapidly $\sim r_{\alpha\beta}^{-3}$ at short distances. Our TPA resonances that depend on coefficients B_3 and B_4 in Eq. (21) are prominent at small atomic separation.

Figure 6 shows the variation of spectra with interatomic distance. For a short distance compared to the wavelength it gives a significant contribution, showing new collective TPA resonances along with strong single-photon resonances. This

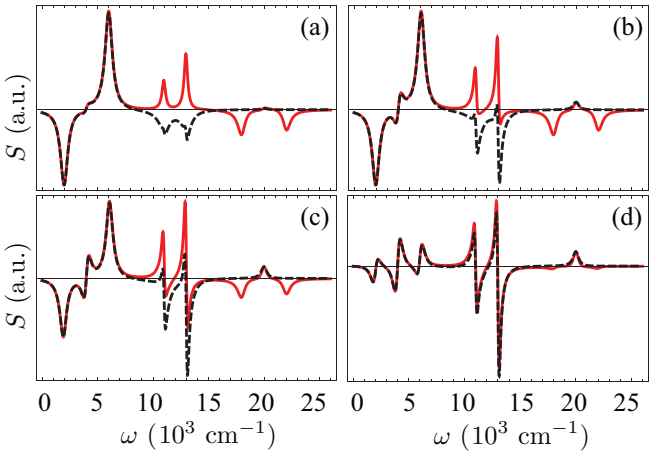

FIG. 6. (Color online) Frequency-dispersed transmission from two atoms with a shaped pulse with zero phase $\xi=0$, $\phi(\omega)=0$, for different distances between atoms $r_{\alpha\beta}/\lambda_a$: (a) 0.001, (b) 0.005, (c) 0.01, and (d) 0.1.

varies at large distances according to Eq. (21). The Raman resonances behave similarly and become weaker with distance in both (20) and (21).

Generally, the QED susceptibility (15) cannot be expressed via the effective coupling through the QME (14). However, in the absence of a bath, setting the ground-state frequency and linewidth to be zero $\omega_g=0$ and $\gamma_g=0$, we have $G_g(\omega)\simeq\delta(\omega)$. Thus both susceptibilities (14) and (15) are governed by the small parameter that is related to the couplings $\mathcal{L}_{\alpha\beta}$ and $\mathcal{M}_{\alpha\beta}$ given by Eqs. (27) and (28), where $|\mathcal{L}_{\alpha\beta}(\omega)|,|\mathcal{M}_{\alpha\beta}(\omega)|\ll|\omega_\alpha-\omega_\beta|,\sigma$, where σ is the bandwidth of the pulse envelopes. As we show below, these couplings enter both QME and QED contributions in different ways.

The magnitude of the QED correction is governed by a combined spectral bandwidth of matter and field degrees of freedom that enter the susceptibilities. This can be best understood in the joint field plus matter space. Due to the consecutive interactions with quantum modes in SC theory, the effective frequency range that enters SC susceptibility (A29)–(A32) is governed by the entire spectrum of quantum modes. In contrast, due to the mixed time ordering of interactions with quantum and classical modes, the effective frequency range that enters the QED susceptibility (A33)–(A35) is limited by a combined classical pulse and matter bandwidth. To illustrate this we note that Eqs. (A29) and (A33) show that for the same set of diagrams (1 and 4 in Fig. 2) the ω_2 dependence enters Eqs. (14) and (15) via $G_\beta(\omega_2)$ and $G_\beta(\omega+\omega_1-\omega_2)$, with $\beta=a,b$, respectively. Therefore, the frequency range of ω_2 in the QED susceptibility is restricted compared to its SC counterpart. Another way to look at it is by noting that the collective resonance in both Eqs. (A29) and (A33) is given by $G_{ab}^{(+)}(\omega+\omega_1)$. Because in the SC signal (A29) the integrations over ω_1 and ω_2 are uncoupled, if a collective resonance exists and is not smeared by the pulse envelope it will enter through the same $G_{ab}^{(+)}(\omega+\omega_1)$. In contrast, due to mixing of the frequency arguments in the QED contribution (A33), integration over ω_2 may give another collective resonance (e.g., $\omega_2=\omega_\alpha-i\gamma_\alpha$) that will

now appear through the product of two Green's functions $G^{(+)}_{ab}(\omega+\omega_1)G_\beta(\omega+\omega_1-\omega_\alpha+i\gamma_\alpha)$, which gives rise to terms such as $G^{(+)2}_{ab}(\omega+\omega_1)$, $G^{(+)2}_{aa}(\omega+\omega_1)$, and $G^{(+)2}_{bb}(\omega+\omega_1)$. In this case, the characteristic coupling accompanying such resonances will be $\tilde{\mathcal{M}}_{\alpha\beta}(\omega_\alpha-i\gamma_\alpha)$ given by Eq. (28), which grows rapidly at small distances. A full QED treatment contains fine details that are missed by the QME.

VII. DISCUSSION

The QME approach has had many successes and is widely used for calculating the third-order response of a collection of two-level atoms. The QME is obtained by a second-order expansion in the field-matter coupling strength, which is equivalent to introducing an effective interatomic coupling. One can further diagonalize the Hamiltonian and take into account the interatomic coupling to all orders. The perturbative QED treatment of the present paper shows that in each order in field-matter coupling there are processes that are missed by the QME.

We have expressed the transmitted signal in terms of a four-point correlation function of the classical fields with an arbitrary number of quantum modes. We presented a QED calculation of the collective resonances to second order in the coupling to quantum vacuum modes. Radiative energy transfer between excited-state populations [34] involves four interactions with the quantum modes (two with A and two with B) and goes beyond the present theory. The QME that is based on the effective coupling stemming from two interactions with quantum mode can describe only certain types of collective resonances (Raman), but not TPA. The QED approach reveals resonant features stemming from nonconsecutive-in-time interactions with quantum modes, i.e., with classical field interaction in between. The magnitude of these contribution is governed by the dipole-dipole coupling and the combined spectral bandwidth of the relevant field and matter degrees of freedom. Generally, the QED contribution to the susceptibility that involves the sum over radiation modes over a restricted frequency range is comparable to the SC susceptibility due to mixed time ordering of interactions. In contrast, the SC susceptibility contains consecutive interactions with quantum modes and thus requires a summation over the entire spectrum of these modes. The use of pulse shaping (the combination of narrowband and broadband pulses) is crucial for observing these collective resonances. These resonances in the transmission of the shaped pulse can be best visualized by two-dimensional plots vs the narrowband and broadband frequencies. The former serves as a frequency reference and the latter is dispersed by the detection. In addition, nonlinear phase shaping involving positive and negative chirp combination allows to eliminate the background and obtain a clear picture of the resonant features that include both collective and single-photon resonances. The pulse phase and amplitude may be used to manipulate the desired resonances.

The present approach is not restricted to classical states of the transmitted pulse and can be easily extended to different types of light, e.g., stochastic or entangled light. These will enter the signal (13) via the four-point correlation function of the incoming field [35,36]. Furthermore, the formalism is not restricted to stimulated signals and can be applied to spontaneous signals as well. One of the potential applications may be to the study of collective vs noncollective features in aggregates with vibronic couplings [37] using photon-counting signals [38,39]. This approach is also applicable to high resolution few molecule studies [40].

ACKNOWLEDGMENTS

The support of the National Science Foundation (Grant No. CHE-1058791), the Chemical Sciences, Geosciences, and Biosciences division, Office of Basic Energy Sciences, Office of Science, US Department of Energy is gratefully acknowledged.

APPENDIX A: SIGNAL CONTRIBUTIONS CORRESPONDING TO FIG. 2

We read off the Liouville pathways from the diagrams in Fig. 2:

$$\begin{aligned}S_{A1}(\omega) = -\mathcal{I}\frac{2i}{\hbar^6}\int_{-\infty}^{\infty}dte^{i\omega t}\int_{-\infty}^{t}d\tau_1\int_{-\infty}^{\tau_1}d\tau_2\int_{-\infty}^{\tau_2}d\tau_3\int_{-\infty}^{\tau_3}d\tau_4\int_{-\infty}^{\tau_4}d\tau_5\int d\mathbf{r}_1d\mathbf{r}_2d\mathbf{r}_3d\mathbf{r}_4d\mathbf{r}_5\\ \times\langle\mathcal{T}E_L^\dagger(\omega,\mathbf{r}_a)E_L^\dagger(\tau_1,\mathbf{r}_1)E_L(\tau_2,\mathbf{r}_2)E_L(\tau_3,\mathbf{r}_3)E_L^\dagger(\tau_4,\mathbf{r}_4)E_L(\tau_5,\mathbf{r}_5)\rangle\\ \times\langle\mathcal{T}V_L(t,\mathbf{r}_a)V_L(\tau_1,\mathbf{r}_1)V_L^\dagger(\tau_2,\mathbf{r}_2)V_L^\dagger(\tau_3,\mathbf{r}_3)V_L(\tau_4,\mathbf{r}_4)V_L^\dagger(\tau_5,\mathbf{r}_5)\rangle,\end{aligned}\tag{A1}$$

$$\begin{aligned}S_{A2}(\omega) = -\mathcal{I}\frac{2i}{\hbar^6}\int_{-\infty}^{\infty}dte^{i\omega t}\int_{-\infty}^{t}d\tau_1\int_{-\infty}^{\tau_1}d\tau_2\int_{-\infty}^{\tau_2}d\tau_3\int_{-\infty}^{\tau_3}d\tau_4\int_{-\infty}^{\tau_4}d\tau_5\int d\mathbf{r}_1d\mathbf{r}_2d\mathbf{r}_3d\mathbf{r}_4d\mathbf{r}_5\\ \times\langle\mathcal{T}E_L^\dagger(\omega,\mathbf{r}_a)E_L(\tau_1,\mathbf{r}_1)E_L^\dagger(\tau_2,\mathbf{r}_2)E_L^\dagger(\tau_3,\mathbf{r}_3)E_L(\tau_4,\mathbf{r}_4)E_L(\tau_5,\mathbf{r}_5)\rangle\\ \times\langle\mathcal{T}V_L(t,\mathbf{r}_a)V_L^\dagger(\tau_1,\mathbf{r}_1)V_L(\tau_2,\mathbf{r}_2)V_L(\tau_3,\mathbf{r}_3)V_L^\dagger(\tau_4,\mathbf{r}_4)V_L^\dagger(\tau_5,\mathbf{r}_5)\rangle,\end{aligned}\tag{A2}$$

$$\begin{aligned}S_{A3}(\omega) = -\mathcal{I}\frac{2i}{\hbar^6}\int_{-\infty}^{\infty}dte^{i\omega t}\int_{-\infty}^{t}d\tau_1\int_{-\infty}^{\tau_1}d\tau_2\int_{-\infty}^{\tau_2}d\tau_3\int_{-\infty}^{\tau_3}d\tau_4\int_{-\infty}^{\tau_4}d\tau_5\int d\mathbf{r}_1d\mathbf{r}_2d\mathbf{r}_3d\mathbf{r}_4d\mathbf{r}_5\\ \times\langle\mathcal{T}E_L^\dagger(\omega,\mathbf{r}_a)E_L^\dagger(\tau_1,\mathbf{r}_1)E_L(\tau_2,\mathbf{r}_2)E_L^\dagger(\tau_3,\mathbf{r}_3)E_L(\tau_4,\mathbf{r}_4)E_L(\tau_5,\mathbf{r}_5)\rangle\\ \times\langle\mathcal{T}V_L(t,\mathbf{r}_a)V_L(\tau_1,\mathbf{r}_1)V_L^\dagger(\tau_2,\mathbf{r}_2)V_L(\tau_3,\mathbf{r}_3)V_L^\dagger(\tau_4,\mathbf{r}_4)V_L^\dagger(\tau_5,\mathbf{r}_5)\rangle,\end{aligned}\tag{A3}$$

$$S_{A4}(\omega) = \mathcal{I}\frac{2i}{\hbar^6}\int_{-\infty}^{\infty} dt e^{i\omega t}\int_{-\infty}^{t} d\tau_1\int_{-\infty}^{\tau_1} d\tau_2\int_{-\infty}^{\tau_2} d\tau_3\int_{-\infty}^{\tau_3} d\tau_4\int_{-\infty}^{t} d\tau_5\int d\mathbf{r}_1 d\mathbf{r}_2 d\mathbf{r}_3 d\mathbf{r}_4 d\mathbf{r}_5$$
$$\times\langle\mathcal{T}E_L^\dagger(\omega,\mathbf{r}_a)E_L(\tau_1,\mathbf{r}_1)E_L(\tau_2,\mathbf{r}_2)E_L^\dagger(\tau_3,\mathbf{r}_3)E_L(\tau_4,\mathbf{r}_4)E_R^\dagger(\tau_5,\mathbf{r}_5)\rangle$$
$$\times\langle\mathcal{T}V_L(t,\mathbf{r}_a)V_L^\dagger(\tau_1,\mathbf{r}_1)V_L^\dagger(\tau_2,\mathbf{r}_2)V_L(\tau_3,\mathbf{r}_3)V_L^\dagger(\tau_4,\mathbf{r}_4)V_R(\tau_5,\mathbf{r}_5)\rangle, \tag{A4}$$

$$S_{A5}(\omega) = \mathcal{I}\frac{2i}{\hbar^6}\int_{-\infty}^{\infty} dt e^{i\omega t}\int_{-\infty}^{t} d\tau_1\int_{-\infty}^{\tau_1} d\tau_2\int_{-\infty}^{\tau_2} d\tau_3\int_{-\infty}^{\tau_3} d\tau_4\int_{-\infty}^{t} d\tau_5\int d\mathbf{r}_1 d\mathbf{r}_2 d\mathbf{r}_3 d\mathbf{r}_4 d\mathbf{r}_5$$
$$\times\langle\mathcal{T}E_L^\dagger(\omega,\mathbf{r}_a)E_L(\tau_1,\mathbf{r}_1)E_L^\dagger(\tau_2,\mathbf{r}_2)E_L(\tau_3,\mathbf{r}_3)E_L(\tau_4,\mathbf{r}_4)E_R^\dagger(\tau_5,\mathbf{r}_5)\rangle$$
$$\times\langle\mathcal{T}V_L(t,\mathbf{r}_a)V_L^\dagger(\tau_1,\mathbf{r}_1)V_L(\tau_2,\mathbf{r}_2)V_L^\dagger(\tau_3,\mathbf{r}_3)V_L^\dagger(\tau_4,\mathbf{r}_4)V_R(\tau_5,\mathbf{r}_5)\rangle, \tag{A5}$$

$$S_{A6}(\omega) = -\mathcal{I}\frac{2i}{\hbar^6}\int_{-\infty}^{\infty} dt e^{i\omega t}\int_{-\infty}^{t} d\tau_1\int_{-\infty}^{\tau_1} d\tau_2\int_{-\infty}^{\tau_2} d\tau_3\int_{-\infty}^{t} d\tau_4\int_{-\infty}^{\tau_4} d\tau_5\int d\mathbf{r}_1 d\mathbf{r}_2 d\mathbf{r}_3 d\mathbf{r}_4 d\mathbf{r}_5$$
$$\times\langle\mathcal{T}E_L^\dagger(\omega,\mathbf{r}_a)E_L^\dagger(\tau_1,\mathbf{r}_1)E_L(\tau_2,\mathbf{r}_2)E_L(\tau_3,\mathbf{r}_3)E_R(\tau_4,\mathbf{r}_4)E_R^\dagger(\tau_5,\mathbf{r}_5)\rangle$$
$$\times\langle\mathcal{T}V_L(t,\mathbf{r}_a)V_L(\tau_1,\mathbf{r}_1)V_L^\dagger(\tau_2,\mathbf{r}_2)V_L^\dagger(\tau_3,\mathbf{r}_3)V_R^\dagger(\tau_4,\mathbf{r}_4)V_R(\tau_5,\mathbf{r}_5)\rangle, \tag{A6}$$

$$S_{A7}(\omega) = \mathcal{I}\frac{2i}{\hbar^6}\int_{-\infty}^{\infty} dt e^{i\omega t}\int_{-\infty}^{t} d\tau_1\int_{-\infty}^{\tau_1} d\tau_2\int_{-\infty}^{t} d\tau_3\int_{-\infty}^{\tau_3} d\tau_4\int_{-\infty}^{\tau_4} d\tau_5\int d\mathbf{r}_1 d\mathbf{r}_2 d\mathbf{r}_3 d\mathbf{r}_4 d\mathbf{r}_5$$
$$\times\langle\mathcal{T}E_L^\dagger(\omega,\mathbf{r}_a)E_L(\tau_1,\mathbf{r}_1)E_L(\tau_2,\mathbf{r}_2)E_R^\dagger(\tau_3,\mathbf{r}_3)E_R(\tau_4,\mathbf{r}_4)E_R^\dagger(\tau_5,\mathbf{r}_5)\rangle$$
$$\times\langle\mathcal{T}V_L(t,\mathbf{r}_a)V_L^\dagger(\tau_1,\mathbf{r}_1)V_L^\dagger(\tau_2,\mathbf{r}_2)V_R(\tau_3,\mathbf{r}_3)V_R^\dagger(\tau_4,\mathbf{r}_4)V_R(\tau_5,\mathbf{r}_5)\rangle. \tag{A7}$$

The above expressions can be recast in Hilbert space:

$$S_{A1}(\omega) = -\mathcal{I}\frac{2i}{\hbar^6}\int_{-\infty}^{\infty} dt e^{i\omega t}\int_{-\infty}^{t} d\tau_1\int_{-\infty}^{\tau_1} d\tau_2\int_{-\infty}^{\tau_2} d\tau_3\int_{-\infty}^{\tau_3} d\tau_4\int_{-\infty}^{\tau_4} d\tau_5\int d\mathbf{r}_1 d\mathbf{r}_2 d\mathbf{r}_3 d\mathbf{r}_4 d\mathbf{r}_5$$
$$\times\langle\mathcal{T}E^\dagger(\omega,\mathbf{r}_a)E^\dagger(\tau_1,\mathbf{r}_1)E(\tau_2,\mathbf{r}_2)E(\tau_3,\mathbf{r}_3)E^\dagger(\tau_4,\mathbf{r}_4)E(\tau_5,\mathbf{r}_5)\rangle$$
$$\times\langle\mathcal{T}V(t,\mathbf{r}_a)V(\tau_1,\mathbf{r}_1)V^\dagger(\tau_2,\mathbf{r}_2)V^\dagger(\tau_3,\mathbf{r}_3)V(\tau_4,\mathbf{r}_4)V^\dagger(\tau_5,\mathbf{r}_5)\rangle, \tag{A8}$$

$$S_{A2}(\omega) = -\mathcal{I}\frac{2i}{\hbar^6}\int_{-\infty}^{\infty} dt e^{i\omega t}\int_{-\infty}^{t} d\tau_1\int_{-\infty}^{\tau_1} d\tau_2\int_{-\infty}^{\tau_2} d\tau_3\int_{-\infty}^{\tau_3} d\tau_4\int_{-\infty}^{\tau_4} d\tau_5\int d\mathbf{r}_1 d\mathbf{r}_2 d\mathbf{r}_3 d\mathbf{r}_4 d\mathbf{r}_5$$
$$\times\langle\mathcal{T}E^\dagger(\omega,\mathbf{r}_a)E(\tau_1,\mathbf{r}_1)E^\dagger(\tau_2,\mathbf{r}_2)E^\dagger(\tau_3,\mathbf{r}_3)E(\tau_4,\mathbf{r}_4)E(\tau_5,\mathbf{r}_5)\rangle$$
$$\times\langle\mathcal{T}V(t,\mathbf{r}_a)V^\dagger(\tau_1,\mathbf{r}_1)V(\tau_2,\mathbf{r}_2)V(\tau_3,\mathbf{r}_3)V^\dagger(\tau_4,\mathbf{r}_4)V^\dagger(\tau_5,\mathbf{r}_5)\rangle, \tag{A9}$$

$$S_{A3}(\omega) = -\mathcal{I}\frac{2i}{\hbar^6}\int_{-\infty}^{\infty} dt e^{i\omega t}\int_{-\infty}^{t} d\tau_1\int_{-\infty}^{\tau_1} d\tau_2\int_{-\infty}^{\tau_2} d\tau_3\int_{-\infty}^{\tau_3} d\tau_4\int_{-\infty}^{\tau_4} d\tau_5\int d\mathbf{r}_1 d\mathbf{r}_2 d\mathbf{r}_3 d\mathbf{r}_4 d\mathbf{r}_5$$
$$\times\langle\mathcal{T}E^\dagger(\omega,\mathbf{r}_a)E^\dagger(\tau_1,\mathbf{r}_1)E(\tau_2,\mathbf{r}_2)E^\dagger(\tau_3,\mathbf{r}_3)E(\tau_4,\mathbf{r}_4)E(\tau_5,\mathbf{r}_5)\rangle$$
$$\times\langle\mathcal{T}V(t,\mathbf{r}_a)V(\tau_1,\mathbf{r}_1)V^\dagger(\tau_2,\mathbf{r}_2)V(\tau_3,\mathbf{r}_3)V^\dagger(\tau_4,\mathbf{r}_4)V^\dagger(\tau_5,\mathbf{r}_5)\rangle, \tag{A10}$$

$$S_{A4}(\omega) = \mathcal{I}\frac{2i}{\hbar^6}\int_{-\infty}^{\infty} dt e^{i\omega t}\int_{-\infty}^{t} d\tau_1\int_{-\infty}^{\tau_1} d\tau_2\int_{-\infty}^{\tau_2} d\tau_3\int_{-\infty}^{\tau_3} d\tau_4\int_{-\infty}^{t} d\tau_5\int d\mathbf{r}_1 d\mathbf{r}_2 d\mathbf{r}_3 d\mathbf{r}_4 d\mathbf{r}_5$$
$$\times\langle\mathcal{T}E^\dagger(\tau_5,\mathbf{r}_5)E^\dagger(\omega,\mathbf{r}_a)E(\tau_1,\mathbf{r}_1)E(\tau_2,\mathbf{r}_2)E^\dagger(\tau_3,\mathbf{r}_3)E(\tau_4,\mathbf{r}_4)\rangle$$
$$\times\langle\mathcal{T}V(\tau_5,\mathbf{r}_5)V(t,\mathbf{r}_a)V^\dagger(\tau_1,\mathbf{r}_1)V^\dagger(\tau_2,\mathbf{r}_2)V(\tau_3,\mathbf{r}_3)V^\dagger(\tau_4,\mathbf{r}_4)\rangle, \tag{A11}$$

$$S_{A5}(\omega) = \mathcal{I}\frac{2i}{\hbar^6}\int_{-\infty}^{\infty} dt e^{i\omega t}\int_{-\infty}^{t} d\tau_1\int_{-\infty}^{\tau_1} d\tau_2\int_{-\infty}^{\tau_2} d\tau_3\int_{-\infty}^{\tau_3} d\tau_4\int_{-\infty}^{t} d\tau_5\int d\mathbf{r}_1 d\mathbf{r}_2 d\mathbf{r}_3 d\mathbf{r}_4 d\mathbf{r}_5$$
$$\times\langle\mathcal{T}E^\dagger(\tau_5,\mathbf{r}_5)E^\dagger(\omega,\mathbf{r}_a)E(\tau_1,\mathbf{r}_1)E^\dagger(\tau_2,\mathbf{r}_2)E(\tau_3,\mathbf{r}_3)E(\tau_4,\mathbf{r}_4)\rangle$$
$$\times\langle\mathcal{T}V(\tau_5,\mathbf{r}_5)V(t,\mathbf{r}_a)V^\dagger(\tau_1,\mathbf{r}_1)V(\tau_2,\mathbf{r}_2)V^\dagger(\tau_3,\mathbf{r}_3)V^\dagger(\tau_4,\mathbf{r}_4)\rangle, \tag{A12}$$

$$S_{A6}(\omega) = -\mathcal{I}\frac{2i}{\hbar^6}\int_{-\infty}^{\infty} dt e^{i\omega t}\int_{-\infty}^{t} d\tau_1\int_{-\infty}^{\tau_1} d\tau_2\int_{-\infty}^{\tau_2} d\tau_3\int_{-\infty}^{t} d\tau_4\int_{-\infty}^{\tau_4} d\tau_5\int d\mathbf{r}_1 d\mathbf{r}_2 d\mathbf{r}_3 d\mathbf{r}_4 d\mathbf{r}_5$$
$$\times\langle\mathcal{T}E^\dagger(\tau_5,\mathbf{r}_5)E(\tau_4,\mathbf{r}_4)E^\dagger(\omega,\mathbf{r}_a)E^\dagger(\tau_1,\mathbf{r}_1)E(\tau_2,\mathbf{r}_2)E(\tau_3,\mathbf{r}_3)\rangle$$
$$\times\langle\mathcal{T}V(\tau_5,\mathbf{r}_5)V^\dagger(\tau_4,\mathbf{r}_4)V(t,\mathbf{r}_a)V(\tau_1,\mathbf{r}_1)V^\dagger(\tau_2,\mathbf{r}_2)V^\dagger(\tau_3,\mathbf{r}_3)\rangle, \tag{A13}$$

$$S_{A7}(\omega) = \mathcal{I}\frac{2i}{\hbar^6}\int_{-\infty}^{\infty} dt e^{i\omega t}\int_{-\infty}^{t} d\tau_1\int_{-\infty}^{\tau_1} d\tau_2\int_{-\infty}^{t} d\tau_3\int_{-\infty}^{\tau_3} d\tau_4\int_{-\infty}^{\tau_4} d\tau_5\int d\mathbf{r}_1 d\mathbf{r}_2 d\mathbf{r}_3 d\mathbf{r}_4 d\mathbf{r}_5$$
$$\times\langle \mathcal{T}E^\dagger(\tau_5,\mathbf{r}_5)E(\tau_4,\mathbf{r}_4)E^\dagger(\tau_3,\mathbf{r}_3)E^\dagger(\omega,\mathbf{r}_a)E(\tau_1,\mathbf{r}_1)E(\tau_2,\mathbf{r}_2)\rangle$$
$$\times\langle \mathcal{T}V(\tau_5,\mathbf{r}_5)V^\dagger(\tau_4,\mathbf{r}_4)V(\tau_3,\mathbf{r}_3)V(t,\mathbf{r}_a)V^\dagger(\tau_1,\mathbf{r}_1)V^\dagger(\tau_2,\mathbf{r}_2)\rangle. \tag{A14}$$

Note that Eqs. (A8)–(A14) contain non-normally ordered correlation functions of the electric field operators and thus contribute to nonclassical features. Since the classical response of a system of noninteracting atoms contains no collective features, we shall focus on the nonclassical signal. These equations can be recast in the frequency domain by expanding the field $E(\tau_j,\mathbf{r}_\alpha) = \int_{-\infty}^{\infty}\frac{d\omega_j}{2\pi}E(\omega_j,\mathbf{r}_\alpha)e^{-i\omega_j\tau_j}$ and taking into account that $V(t,\mathbf{r}) = \sum_\alpha \mathbf{V}^\alpha(t)\delta(\mathbf{r}-\mathbf{r}_\alpha)$, $\alpha = a,b$:

$$S_{A1}(\omega) = -\mathcal{I}\frac{2i}{\hbar^6}\sum_{\alpha,\beta}\int_{-\infty}^{\infty}\frac{d\omega_1}{2\pi}\frac{d\omega_2}{2\pi}\frac{d\omega_3}{2\pi}\frac{d\omega_4}{2\pi}\frac{d\omega_5}{2\pi}\{\langle E^\dagger(\omega,\mathbf{r}_a)E^\dagger(\omega_1,\mathbf{r}_b)E(\omega_2,\mathbf{r}_{\bar\beta})E(\omega_5,\mathbf{r}_\alpha)\rangle[E(\omega_3,\mathbf{r}_\beta),E^\dagger(\omega_4,\mathbf{r}_\alpha)]$$
$$+\langle E^\dagger(\omega,\mathbf{r}_a)E^\dagger(\omega_1,\mathbf{r}_b)E(\omega_3,\mathbf{r}_\beta)E(\omega_5,\mathbf{r}_\alpha)\rangle[E(\omega_2,\mathbf{r}_{\bar\beta}),E^\dagger(\omega_4,\mathbf{r}_\alpha)]\}R_{A1}^{(\alpha\beta)}(\omega,\omega_1,\omega_2,\omega_3,\omega_4,\omega_5), \tag{A15}$$

$$S_{A2}(\omega) = -\mathcal{I}\frac{2i}{\hbar^6}\sum_{\alpha,\beta}\int_{-\infty}^{\infty}\frac{d\omega_1}{2\pi}\frac{d\omega_2}{2\pi}\frac{d\omega_3}{2\pi}\frac{d\omega_4}{2\pi}\frac{d\omega_5}{2\pi}\{\langle E^\dagger(\omega,\mathbf{r}_a)E^\dagger(\omega_2,\mathbf{r}_\beta)E(\omega_4,\mathbf{r}_{\bar\alpha})E(\omega_5,\mathbf{r}_\alpha)\rangle[E(\omega_1,\mathbf{r}_a),E^\dagger(\omega_3,\mathbf{r}_{\bar\beta})]$$
$$+\langle E^\dagger(\omega,\mathbf{r}_a)E^\dagger(\omega_3,\mathbf{r}_{\bar\beta})E(\omega_4,\mathbf{r}_{\bar\alpha})E(\omega_5,\mathbf{r}_\alpha)\rangle[E(\omega_1,\mathbf{r}_a),E^\dagger(\omega_2,\mathbf{r}_\beta)]\}R_{A2}^{(\alpha\beta)}(\omega,\omega_1,\omega_2,\omega_3,\omega_4,\omega_5), \tag{A16}$$

$$S_{A3}(\omega) = -\mathcal{I}\frac{2i}{\hbar^6}\sum_{\alpha,\beta}\int_{-\infty}^{\infty}\frac{d\omega_1}{2\pi}\frac{d\omega_2}{2\pi}\frac{d\omega_3}{2\pi}\frac{d\omega_4}{2\pi}\frac{d\omega_5}{2\pi}\langle E^\dagger(\omega,\mathbf{r}_a)E^\dagger(\omega_1,\mathbf{r}_b)E(\omega_4,\mathbf{r}_{\bar\alpha})E(\omega_5,\mathbf{r}_\alpha)\rangle[E(\omega_2,\mathbf{r}_{\bar\beta}),E^\dagger(\omega_3,\mathbf{r}_{\bar\beta})]$$
$$\times R_{A3}^{(\alpha\beta)}(\omega,\omega_1,\omega_2,\omega_3,\omega_4,\omega_5), \tag{A17}$$

$$S_{A4}(\omega) = \mathcal{I}\frac{2i}{\hbar^6}\sum_{\alpha,\beta}\int_{-\infty}^{\infty}\frac{d\omega_1}{2\pi}\frac{d\omega_2}{2\pi}\frac{d\omega_3}{2\pi}\frac{d\omega_4}{2\pi}\frac{d\omega_5}{2\pi}\{\langle E^\dagger(\omega_5,\mathbf{r}_b)E^\dagger(\omega,\mathbf{r}_a)E(\omega_2,\mathbf{r}_\beta)E(\omega_4,\mathbf{r}_\alpha)\rangle[E(\omega_1,\mathbf{r}_{\bar\beta}),E^\dagger(\omega_3,\mathbf{r}_\alpha)]$$
$$+\langle E^\dagger(\omega_5,\mathbf{r}_b)E^\dagger(\omega,\mathbf{r}_a)E(\omega_1,\mathbf{r}_{\bar\beta})E(\omega_4,\mathbf{r}_\alpha)\rangle[E(\omega_2,\mathbf{r}_\beta),E^\dagger(\omega_3,\mathbf{r}_\alpha)]\}R_{A4}^{(\alpha\beta)}(\omega,\omega_1,\omega_2,\omega_3,\omega_4,\omega_5), \tag{A18}$$

$$S_{A5}(\omega) = \mathcal{I}\frac{2i}{\hbar^6}\sum_{\alpha,\beta}\int_{-\infty}^{\infty}\frac{d\omega_1}{2\pi}\frac{d\omega_2}{2\pi}\frac{d\omega_3}{2\pi}\frac{d\omega_4}{2\pi}\frac{d\omega_5}{2\pi}\langle E^\dagger(\omega_5,\mathbf{r}_b)E^\dagger(\omega,\mathbf{r}_a)E(\omega_3,\mathbf{r}_{\bar\alpha})E(\omega_4,\mathbf{r}_\alpha)\rangle[E(\omega_1,\mathbf{r}_{\bar\beta}),E^\dagger(\omega_2,\mathbf{r}_{\bar\beta})]$$
$$\times R_{A5}^{(\alpha\beta)}(\omega,\omega_1,\omega_2,\omega_3,\omega_4,\omega_5), \tag{A19}$$

$$S_{A6}(\omega) = -\mathcal{I}\frac{2i}{\hbar^6}\sum_{\alpha,\beta}\int_{-\infty}^{\infty}\frac{d\omega_1}{2\pi}\frac{d\omega_2}{2\pi}\frac{d\omega_3}{2\pi}\frac{d\omega_4}{2\pi}\frac{d\omega_5}{2\pi}\langle E^\dagger(\omega_5,\mathbf{r}_\beta)E^\dagger(\omega,\mathbf{r}_a)E(\omega_2,\mathbf{r}_{\bar\alpha})E(\omega_3,\mathbf{r}_\alpha)\rangle[E(\omega_4,\mathbf{r}_\beta),E^\dagger(\omega_1,\mathbf{r}_b)]$$
$$\times R_{A6}^{(\alpha\beta)}(\omega,\omega_1,\omega_2,\omega_3,\omega_4,\omega_5), \tag{A20}$$

$$S_{A7}(\omega) = \mathcal{I}\frac{2i}{\hbar^6}\sum_{\alpha,\beta}\int_{-\infty}^{\infty}\frac{d\omega_1}{2\pi}\frac{d\omega_2}{2\pi}\frac{d\omega_3}{2\pi}\frac{d\omega_4}{2\pi}\frac{d\omega_5}{2\pi}\langle E^\dagger(\omega_5,\mathbf{r}_\beta)E^\dagger(\omega,\mathbf{r}_a)E(\omega_1,\mathbf{r}_{\bar\alpha})E(\omega_2,\mathbf{r}_\alpha)\rangle[E(\omega_4,\mathbf{r}_\beta),E^\dagger(\omega_3,\mathbf{r}_b)]$$
$$\times R_{A7}^{(\alpha\beta)}(\omega,\omega_1,\omega_2,\omega_3,\omega_4,\omega_5). \tag{A21}$$

Here

$$R_{A1}^{(\alpha\beta)}(\omega,\omega_1,\omega_2,\omega_3,\omega_4,\omega_5) = 2\pi|\mu_\alpha|^2\mu_\beta^*\mu_{\bar\beta}^*\mu_a\mu_b\delta(\omega+\omega_1-\omega_2-\omega_3+\omega_4-\omega_5)G_{ab}^{(+)}(\omega+\omega_1)$$
$$\times G_a(\omega)G_\alpha(\omega_5)G_\beta(\omega+\omega_1-\omega_2)G_g(\omega_5-\omega_4), \tag{A22}$$

$$R_{A2}^{(\alpha\beta)}(\omega,\omega_1,\omega_2,\omega_3,\omega_4,\omega_5) = 2\pi\mu_\alpha^*\mu_{\bar\alpha}^*\mu_{\bar\beta}\mu_\beta|\mu_a|^2\delta(\omega-\omega_1+\omega_2+\omega_3-\omega_4-\omega_5)G_{ab}^{(+)}(\omega_4+\omega_5)$$
$$\times G_a(\omega)G_\alpha(\omega_5)G_\beta(\omega+\omega_2-\omega_1)G_g(\omega_4+\omega_5-\omega_2-\omega_3), \tag{A23}$$

$$R_{A3}^{(\alpha\beta)}(\omega,\omega_1,\omega_2,\omega_3,\omega_4,\omega_5) = 2\pi\mu_\alpha^*\mu_{\bar\alpha}^*|\mu_{\bar\beta}|^2\mu_a\mu_b\delta(\omega+\omega_1-\omega_2+\omega_3-\omega_4-\omega_5)G_{ab}^{(+)}(\omega_4+\omega_5)G_{ab}^{(+)}(\omega+\omega_1)$$
$$\times G_a(\omega)G_\beta(\omega+\omega_1-\omega_2)G_\alpha(\omega_5), \tag{A24}$$

$$R_{A4}^{(\alpha\beta)}(\omega,\omega_1,\omega_2,\omega_3,\omega_4,\omega_5) = 2\pi\mu_\beta^*\mu_{\bar\beta}^*|\mu_\alpha|^2\mu_a\mu_b\delta(\omega-\omega_1-\omega_2+\omega_3-\omega_4+\omega_5)G_{ab}^{(+)}(\omega+\omega_5)$$
$$\times G_b^\dagger(\omega_5)G_\beta(\omega_2+\omega_4-\omega_3)G_\alpha(\omega_4)G_g(\omega_4-\omega_3), \tag{A25}$$

$$R^{(\alpha\beta)}_{A5}(\omega,\omega_1,\omega_2,\omega_3,\omega_4,\omega_5) = 2\pi\mu^*_\alpha\mu^*_{\bar\alpha}|\mu_{\bar\beta}|^2\mu_a\mu_b\delta(\omega-\omega_1+\omega_2-\omega_3-\omega_4+\omega_5)G^{(+)}_{ab}(\omega_3+\omega_4)G^{(+)}_{ab}(\omega+\omega_5)$$
$$\times G^\dagger_b(\omega_5)G_\beta(\omega+\omega_5-\omega_1)G_\alpha(\omega_4), \tag{A26}$$

$$R^{(\alpha\beta)}_{A6}(\omega,\omega_1,\omega_2,\omega_3,\omega_4,\omega_5) = 2\pi\mu^*_\alpha\mu^*_{\bar\alpha}|\mu_\beta|^2\mu_a\mu_b\delta(\omega+\omega_1-\omega_2-\omega_3-\omega_4+\omega_5)G^{(+)}_{ab}(\omega_2+\omega_3)$$
$$\times G_a(\omega+\omega_5-\omega_4)G^\dagger_\beta(\omega_5)G_\alpha(\omega_3)G_g(\omega_5-\omega_4), \tag{A27}$$

$$R^{(\alpha\beta)}_{A7}(\omega,\omega_1,\omega_2,\omega_3,\omega_4,\omega_5) = 2\pi\mu^*_\alpha\mu^*_{\bar\alpha}|\mu_\beta|^2\mu_a\mu_b\delta(\omega-\omega_1-\omega_2+\omega_3-\omega_4+\omega_5)G^{(+)}_{ab}(\omega_1+\omega_2)$$
$$\times G^\dagger_b(-\omega+\omega_1+\omega_2)G^\dagger_\beta(\omega_5)G_\alpha(\omega_2)G^\dagger_g(\omega_5-\omega_4). \tag{A28}$$

Note that due to permutations $\alpha,\beta = a,b$ a single diagram in Fig. 2 represents four single-quantum pathways. Pathways (A22)–(A28) contribute for both SC and QED results that differ by a field correlation function. We also note that the field part consists of a commutator that involves two quantum modes and a four-point correlation function of the classical field. The latter is simply a product of four classical amplitudes. The former can be calculated using the commutation relations (6) and (7). Performing the frequency integrations, we obtain the signal (13) with nonlinear susceptibilities given by Eq. (14) where

$$\left[\chi^{(3)I}_{1LLLL}+\chi^{(3)I}_{4LLLR}+\chi^{(3)I}_{4(L\leftrightarrow R)}\right](-\omega,-\omega_1,\omega+\omega_1-\omega_2,\omega_2)$$
$$= G^{(+)}_{ab}(\omega+\omega_1)[G^\dagger_s(\omega_1)-G_s(\omega)]\sum_{\alpha,\beta}\tilde{\mathcal{L}}_{\alpha\beta}(\omega_2)e^{-i\mathbf{k}_0(\mathbf{r}_\alpha-\mathbf{r}_\beta)}G_\alpha(\omega_2)G_\beta(\omega_2), \tag{A29}$$

$$\chi^{(3)I}_{3LLLL}(-\omega,-\omega_1,\omega+\omega_1-\omega_2,\omega_2)+\left[\chi^{(3)I}_{5LLLR}+\chi^{(3)I}_{5(L\leftrightarrow R)}\right](-\omega,-\omega_1,\omega+\omega_1-\omega_2,\omega_2)$$
$$= G^{(+)2}_{ab}(\omega+\omega_1)[G^\dagger_s(\omega_1)-G_s(\omega)]\mathcal{L}_s(\omega+\omega_1)G_s(\omega+\omega_1-\omega_2), \tag{A30}$$

$$\chi^{(3)I}_{2LLLL}(-\omega,-\omega_1,\omega+\omega_1-\omega_2,\omega_2) = -G^{(+)}_{ab}(\omega+\omega_1)G_s(\omega+\omega_1-\omega_2)\sum_{\alpha,\beta}\mathcal{L}_{\alpha\beta}(\omega)e^{-i\mathbf{k}_0(\mathbf{r}_\alpha-\mathbf{r}_\beta)}G_\alpha(\omega)G_\beta(\omega), \tag{A31}$$

$$\left[\chi^{(3)I}_{7LLLR}+\chi^{(3)I}_{7(L\leftrightarrow R)}\right](-\omega,-\omega_1,\omega+\omega_1-\omega_2,\omega_2) = G^{(+)}_{ab}(\omega+\omega_1)G_s(\omega+\omega_1-\omega_2)\sum_{\alpha,\beta}\mathcal{L}_{\alpha\beta}(\omega_1)e^{-i\mathbf{k}_0(\mathbf{r}_\alpha-\mathbf{r}_\beta)}G^\dagger_\alpha(\omega_1)G^\dagger_\beta(\omega_1), \tag{A32}$$

where the couplings $\mathcal{L}_{\alpha\beta}(\omega)$ and $\mathcal{L}_s(\omega+\omega_1)$ are given by Eqs. (24) and (25), respectively, $\tilde{\mathcal{L}}_{\alpha\beta}(\omega) = \mathcal{L}_{\alpha\beta}(\omega)|\mu_\beta|^2/|\mu_\alpha|^2$, and $G_s(\omega) = G_a(\omega)+G_b(\omega)$. Similarly, we evaluate the QED contribution to the susceptibility and get

$$\left[\chi^{(5)II}_{1LLLLLL}+\chi^{(5)II}_{4LLLLLR}+\chi^{(5)II}_{4(L\leftrightarrow R)}\right](-\omega,-\omega_1,\omega',\omega+\omega_1-\omega_2,-\omega',\omega_2)$$
$$= G^{(+)}_{ab}(\omega+\omega_1)[G^\dagger_s(\omega_1)-G_s(\omega)]\sum_{\alpha,\beta}e^{-i\mathbf{k}_0(\mathbf{r}_\alpha-\mathbf{r}_\beta)}\mu^{(l)*}_\beta\mu^{(m)}_\alpha\mathcal{D}^{(l,m)}_{\alpha\beta}(\omega')G_g(\omega_2-\omega')G_\alpha(\omega_2)G_\beta(\omega+\omega_1-\omega'), \tag{A33}$$

$$\chi^{(5)II}_{2LLLLLL}(-\omega,\omega',-\omega_1,-\omega',\omega+\omega_1-\omega_2,\omega_2)$$
$$= -G^{(+)}_{ab}(\omega+\omega_1)G_s(\omega+\omega_1-\omega_2)\sum_{\alpha,\beta}e^{-i\mathbf{k}_0(\mathbf{r}_\alpha-\mathbf{r}_\beta)}\mu^{(l)*}_\alpha\mu^{(m)}_\beta\mathcal{D}^{(l,m)}_{\alpha\beta}(\omega')G_g(\omega-\omega')\mathcal{L}_{\alpha\beta}(\omega)G_\alpha(\omega)G_\beta(\omega+\omega_1-\omega'), \tag{A34}$$

$$\left[\chi^{(5)II}_{6LLLLRR}+\chi^{(5)II}_{6(L\leftrightarrow R)}\right](-\omega,\omega',-\omega_1,-\omega',\omega+\omega_1-\omega_2,\omega_2)$$
$$= -G^{(+)}_{ab}(\omega+\omega_1)G_s(\omega_2)\sum_{\alpha,\beta}e^{-i\mathbf{k}_0(\mathbf{r}_\alpha-\mathbf{r}_\beta)}\mu^{(l)*}_\alpha\mu^{(m)}_\beta\mathcal{D}^{(l,m)}_{\alpha\beta}(\omega')G_g(\omega_1-\omega')G^\dagger_\alpha(\omega_1)G_\beta(\omega+\omega_1-\omega'). \tag{A35}$$

In the absence of the bath, assuming the ground-state frequency and linewidth to be zero $\omega_g = 0$ and $\gamma_g = 0$, we have $G_g(\omega) \simeq \delta(\omega)$.

APPENDIX B: TRANSMISSION OF SHAPED PULSES

Substituting susceptibilities (A29)–(A35) into the signal (13) and utilizing the pulse shaping in the field correlation function (17), we obtain for the semiclassical contribution (20), where

$$A_1(\omega,\omega_p) = [G^\dagger_s(\omega_p)-G_s(\omega)]\int_{-\infty}^{\infty}d\omega_2 e^{i[\phi(\omega+\omega_p-\omega_2)+\phi(\omega_2)-\phi(\omega)-\xi]}\sum_{\alpha,\beta}\tilde{\mathcal{L}}_{\alpha\beta}(\omega_2)e^{-i\mathbf{k}_0(\mathbf{r}_\alpha-\mathbf{r}_\beta)}G_\alpha(\omega_2)G_\beta(\omega_2)$$
$$-2\pi\sum_\alpha e^{i[\phi(\omega_\alpha-i\gamma_\alpha)+\phi(\omega+\omega_p-\omega_\alpha+i\gamma_\alpha)-\phi(\omega)-\xi]}\sum_{\beta,\delta}e^{-i\mathbf{k}_0(\mathbf{r}_\beta-\mathbf{r}_\delta)}[\mathcal{L}_{\beta\delta}(\omega)G_\beta(\omega)G_\delta(\omega)-\mathcal{L}_{\beta\delta}(\omega_p)G^\dagger_\beta(\omega_p)G^\dagger_\delta(\omega_p)], \tag{B1}$$

$$A_2(\omega,\omega_p) = 2\pi[G^\dagger_s(\omega_p)-G_s(\omega)]\sum_\alpha e^{i[\phi(\omega_\alpha-i\gamma_\alpha)+\phi(\omega+\omega_p-\omega_\alpha+i\gamma_\alpha)-\phi(\omega)-\xi]}\mathcal{L}_s(\omega+\omega_p), \tag{B2}$$

$$A_3^{(\alpha)}(\omega,\omega_p) = 2\pi e^{i[\phi(\omega-\omega_p+\omega_\alpha+i\gamma_\alpha)+\xi-\phi(\omega_\alpha+i\gamma_\alpha)-\phi(\omega)]} G_{\bar{\alpha}}^2(\omega)\mathcal{L}_s(\omega+\omega_\alpha+i\gamma_\alpha), \tag{B3}$$

$$A_4^{(\alpha\beta\gamma)}(\omega,\omega_p) = 2\pi e^{i[\phi(\omega-\omega_p+\omega_\alpha+i\gamma_\alpha)+\xi-\phi(\omega_\alpha+i\gamma_\alpha)-\phi(\omega)]} G_{\bar{\alpha}}(\omega)\mathcal{M}_{\beta\delta}(\omega-\omega_p+\omega_\alpha+i\gamma_\alpha)e^{-i\mathbf{k}_0(\mathbf{r}_\beta-\mathbf{r}_\delta)}, \tag{B4}$$

$$A_5^{(\alpha\beta\gamma)}(\omega,\omega_p) = 2\pi e^{i[-\phi(\omega_p-\omega+\omega_\alpha-i\gamma_\alpha)+\xi+\phi(\omega_\alpha-i\gamma_\alpha)-\phi(\omega)]} G_{\bar{\alpha}}(\omega_p)\mathcal{M}_{\beta\delta}(\omega_p-\omega+\omega_\alpha-i\gamma_\alpha)e^{-i\mathbf{k}_0(\mathbf{r}_\beta-\mathbf{r}_\delta)}, \tag{B5}$$

$$\begin{aligned} A_6(\omega,\omega_p) = {} & [G_s^\dagger(\omega_p)-G_s(\omega)]\sum_{\alpha,\beta}\tilde{\mathcal{L}}_{\alpha\beta}(\omega)e^{-i\mathbf{k}_0(\mathbf{r}_\alpha-\mathbf{r}_\beta)}G_\alpha(\omega)G_\beta(\omega) \\ & + [G_s(\omega)+G_s(\omega_p)]\Bigg[\sum_{\alpha,\beta}\mathcal{L}_{\alpha\beta}(\omega_p)e^{-i\mathbf{k}_0(\mathbf{r}_\alpha-\mathbf{r}_\beta)}G_\alpha^\dagger(\omega_p)G_\beta^\dagger(\omega_p)-1\Bigg], \end{aligned} \tag{B6}$$

$$\begin{aligned} A_7(\omega,\omega_p) = {} & e^{i[2\xi-\phi(\omega)-\phi(2\omega_p-\omega)]}[G_s^\dagger(2\omega_p-\omega)-G_s(\omega)]\sum_{\alpha,\beta}\tilde{\mathcal{L}}_{\alpha\beta}(\omega)e^{-i\mathbf{k}_0(\mathbf{r}_\alpha-\mathbf{r}_\beta)}G_\alpha(\omega)G_\beta(\omega) \\ & + e^{i[2\xi-\phi(\omega)-\phi(2\omega_p-\omega)]}G_s(2\omega_p-\omega)\Bigg[\sum_{\alpha,\beta}\mathcal{L}_{\alpha\beta}(2\omega_p-\omega)e^{-i\mathbf{k}_0(\mathbf{r}_\alpha-\mathbf{r}_\beta)}G_\alpha^\dagger(2\omega_p-\omega)G_\beta^\dagger(2\omega_p-\omega)-1\Bigg], \end{aligned} \tag{B7}$$

$$A_8(\omega,\omega_p) = [G_s^\dagger(\omega_p)-G_s(\omega)][G_s(\omega)+G_s(\omega_p)]L_s(\omega+\omega_p), \tag{B8}$$

$$A_9(\omega,\omega_p) = [G_s^\dagger(2\omega_p-\omega)-G_s(\omega)]G_s(2\omega_p-\omega)\mathcal{L}_s(2\omega_p)e^{i[2\xi-\phi(\omega)-\phi(2\omega_p-\omega)]}. \tag{B9}$$

Similarly for the QED contribution, we obtain Eq. (21), where

$$B_1(\omega,\omega_p) = -2\pi\sum_{\alpha,\beta,\delta}e^{i[\phi(\omega+\omega_p-\omega_\alpha+i\gamma_\alpha)+\phi(\omega_\alpha-i\gamma_\alpha)-\phi(\omega)-\xi]}\mathcal{L}_{\beta\delta}(\omega)e^{-i\mathbf{k}_0(\mathbf{r}_\beta-\mathbf{r}_\delta)}[G_\beta(\omega)G_{\bar{\delta}}(\omega_p)+G_\beta^\dagger(\omega_p)G_{\bar{\delta}}(\omega)], \tag{B10}$$

$$B_2(\omega,\omega_p) = 2\pi[G_s^\dagger(\omega_p)-G_s(\omega)]\sum_\alpha\tilde{\mathcal{L}}_{\alpha\alpha}(\omega_\alpha-i\gamma_\alpha)e^{i[\phi(\omega+\omega_p-\omega_\alpha+i\gamma_\alpha)+\phi(\omega_\alpha-i\gamma_\alpha)-\phi(\omega)-\xi]}, \tag{B11}$$

$$B_3(\omega,\omega_p) = 2\pi[G_s^\dagger(\omega_p)-G_s(\omega)]\tilde{\mathcal{M}}_{ba}(\omega_a-i\gamma_a)e^{-i\mathbf{k}_0(\mathbf{r}_b-\mathbf{r}_a)}e^{i[\phi(\omega+\omega_p-\omega_a+i\gamma_a)+\phi(\omega_a-i\gamma_a)-\phi(\omega)-\xi]}, \tag{B12}$$

$$B_4(\omega,\omega_p) = 2\pi[G_s^\dagger(\omega_p)-G_s(\omega)]\tilde{\mathcal{M}}_{ab}(\omega_b-i\gamma_b)e^{-i\mathbf{k}_0(\mathbf{r}_a-\mathbf{r}_b)}e^{i[\phi(\omega+\omega_p-\omega_b+i\gamma_b)+\phi(\omega_b-i\gamma_b)-\phi(\omega)-\xi]}, \tag{B13}$$

$$\begin{aligned} B_5^{(\alpha\beta)}(\omega,\omega_p) = {} & 2\pi G_{\bar{\alpha}}(\omega)e^{i[\phi(\omega-\omega_p+\omega_\alpha+i\gamma_\alpha)+\xi-\phi(\omega)-\phi(\omega_\alpha+i\gamma_\alpha)]}\{[\tilde{\mathcal{L}}_{\bar{\beta}\bar{\beta}}(\omega_p)+\tilde{\mathcal{M}}_{\beta\beta}(\omega-\omega_p+\omega_\alpha+i\gamma_\alpha)]G_{\bar{\beta}}(\omega_p) \\ & + [\tilde{\mathcal{L}}_{\bar{\beta}\beta}(\omega_p)+\tilde{\mathcal{M}}_{\bar{\beta}\beta}(\omega-\omega_p+\omega_\alpha+i\gamma_\alpha)e^{-i\mathbf{k}_0(\mathbf{r}_{\bar{\beta}}-\mathbf{r}_\beta)}]G_\beta(\omega_p)\} \\ & - 2\pi G_{\bar{\alpha}}(\omega)e^{i[\phi(\omega-\omega_p+\omega_\alpha-i\gamma_\alpha)+\xi-\phi(\omega)-\phi(\omega_\alpha-i\gamma_\alpha)]}[\mathcal{L}_{\bar{\alpha}\bar{\alpha}}(\omega)G_{\bar{\alpha}}(\omega)+\mathcal{L}_{\alpha\bar{\alpha}}(\omega)G_\alpha(\omega)], \end{aligned} \tag{B14}$$

$$B_6^{(\alpha\beta)}(\omega,\omega_p) = -2\pi G_{\bar{\alpha}}(\omega_p)e^{i[-\phi(\omega_p-\omega+\omega_\alpha-i\gamma_\alpha)+\phi(\omega_\alpha-i\gamma_\alpha)+\xi-\phi(\omega)]}[\mathcal{L}_{\bar{\beta}\bar{\beta}}(\omega)G_{\bar{\beta}}(\omega)+\mathcal{L}_{\beta\bar{\beta}}(\omega)e^{-i\mathbf{k}_0(\mathbf{r}_\beta-\mathbf{r}_{\bar{\beta}})}G_\beta(\omega)], \tag{B15}$$

$$\begin{aligned} B_7^{(\alpha\beta)}(\omega,\omega_p) = {} & -2\pi G_{\bar{\alpha}}(\omega_p)e^{i[-\phi(\omega_p-\omega+\omega_\alpha-i\gamma_\alpha)+\phi(\omega_\alpha-i\gamma_\alpha)+\xi-\phi(\omega)]} \\ & \times[\mathcal{M}_{\beta\beta}(\omega_p-\omega+\omega_\alpha-i\gamma_\alpha)G_{\bar{\beta}}(\omega)+\mathcal{M}_{\beta\bar{\beta}}(\omega_p-\omega+\omega_\alpha-i\gamma_\alpha)e^{-i\mathbf{k}_0(\mathbf{r}_\beta-\mathbf{r}_{\bar{\beta}})}G_\beta(\omega)], \end{aligned} \tag{B16}$$

$$\begin{aligned} B_8(\omega,\omega_p) = {} & [G_s^\dagger(\omega_p)-G_s(\omega)]\sum_{\alpha,\beta}[\tilde{\mathcal{L}}_{\alpha\beta}(\omega)G_\alpha(\omega)G_{\bar{\beta}}(\omega_p)+\tilde{\mathcal{L}}_{\alpha\beta}(\omega_p)G_{\bar{\alpha}\beta}(\omega)G_\beta(\omega_p)]e^{-i\mathbf{k}_0(\mathbf{r}_\alpha-\mathbf{r}_\beta)} \\ & - [G_s(\omega_p)+G_s(\omega)]\sum_{\alpha,\beta}[\mathcal{L}_{\alpha\beta}(\omega)G_\alpha(\omega)G_{\bar{\beta}}(\omega_p)+\mathcal{L}_{\alpha\beta}(\omega_p)G_\alpha^\dagger(\omega_p)G_{\bar{\beta}}(\omega)]e^{-i\mathbf{k}_0(\mathbf{r}_\alpha-\mathbf{r}_\beta)}, \end{aligned} \tag{B17}$$

$$\begin{aligned} B_9(\omega,\omega_p) = {} & e^{i[2\xi-\phi(\omega)-\phi(2\omega_p-\omega)]}\Bigg([G_s^\dagger(2\omega_p-\omega)-G_s(\omega)]\sum_{\alpha,\beta}\tilde{\mathcal{L}}_{\alpha\beta}(\omega)e^{-i\mathbf{k}_0(\mathbf{r}_\alpha-\mathbf{r}_\beta)}G_{\bar{\alpha}}(2\omega_p-\omega)G_\beta(\omega) \\ & - G_s(2\omega_p-\omega)\sum_{\alpha,\beta}[\mathcal{L}_{\alpha\beta}(\omega)G_\alpha(\omega)G_{\bar{\beta}}(2\omega_p-\omega)+\mathcal{L}_{\alpha\beta}(2\omega_p-\omega)G_\alpha^\dagger(2\omega_p-\omega)G_{\bar{\beta}}(\omega)]e^{-i\mathbf{k}_0(\mathbf{r}_\alpha-\mathbf{r}_\beta)}\Bigg). \end{aligned} \tag{B18}$$

In the above expressions the couplings are given by Eqs. (27) and (28) and $\tilde{\mathcal{L}}_{\alpha\beta}(\omega)=\mathcal{L}_{\alpha\beta}(\omega)|\mu_\beta|^2/|\mu_\alpha|^2$ and $\tilde{\mathcal{M}}_{\alpha\beta}(\omega)=\mathcal{M}_{\alpha\beta}(\omega)|\mu_\beta|^2/|\mu_\alpha|^2$.

[1] D. N. Basov, R. D. Averitt, D. van der Marel, M. Dressel, and K. Haule, Rev. Mod. Phys. **83**, 471 (2011).

[2] A. I. Kuleff and L. S. Cederbaum, Phys. Rev. Lett. **106**, 053001 (2011).

[3] J. Orenstein, Phys. Today **65** (9), 44 (2012).

[4] H. Haug and S. Koch, *Quantum Theory of the Optical and Electronic Properties of Semiconductors* (World Scientific, Singapore, 2004).

[5] G. Mahan, *Condensed Matter in a Nutshell* (Princeton University Press, Princeton, 2011).

[6] S. Mukamel, *Principles of Nonlinear Optical Spectroscopy*, 1st ed. (Oxford University Press, New York, 1995).

[7] Y.-C. Cheng and G. R. Fleming, Annu. Rev. Phys. Chem. **60**, 241 (2009).

[8] E. Collini, C. Wong, K. Wilk, P. Curmi, P. Brumer, and G. D. Scholes, Nature (London) **463**, 644 (2010).

[9] K. E. Dorfman, D. V. Voronine, S. Mukamel, and M. O. Scully, Proc. Natl. Acad. Sci. USA **110**, 2746 (2013).

[10] H. Van Amerongen, L. Valkūnas, and R. Van Grondelle, *Photosynthetic Excitons* (World Scientific, Singapore, 2000).

[11] M. Nielsen and I. Chuang, *Quantum Computation and Quantum Information*, Cambridge Series on Information and the Natural Sciences (Cambridge University Press, Cambridge, 2000).

[12] M. D. Lukin, M. Fleischhauer, R. Cote, L. M. Duan, D. Jaksch, J. I. Cirac, and P. Zoller, Phys. Rev. Lett. **87**, 037901 (2001).

[13] A. Salam, *Molecular Quantum Electrodynamics: Long-Range Intermolecular Interactions* (Wiley, Hoboken, NJ, 2010).

[14] E. A. Power and T. Thirunamachandran, Proc. R. Soc. London Ser. A **372**, 265 (1980).

[15] E. A. Power and T. Thirunamachandran, Phys. Rev. A **26**, 1800 (1982).

[16] D. Craig and T. Thirunamachandran, *Molecular Quantum Electrodynamics: An Introduction to Radiation-Molecule Interactions*, Dover Books on Chemistry Series (Dover, New York, 1984).

[17] M. Wollenhaupt, A. Assion, and T. Baumert, in *Springer Handbook of Lasers and Optics*, edited by F. Träger (Springer, New York, 2007), pp. 937–983.

[18] I. A. Walmsley and C. Dorrer, Adv. Opt. Photon. **1**, 308 (2009).

[19] D. Pestov, R. K. Murawski, G. O. Ariunbold, X. Wang, M. Zhi, A. V. Sokolov, V. A. Sautenkov, Y. V. Rostovtsev, A. Dogariu, Y. Huang, and M. O. Scully, Science **316**, 265 (2007).

[20] X. Wang, A. Zhang, M. Zhi, A. V. Sokolov, G. R. Welch, and M. O. Scully, Opt. Lett. **35**, 721 (2010).

[21] S. Roy, P. J. Wrzesinski, D. Pestov, M. Dantus, and J. R. Gord, J. Raman Spectrosc. **41**, 1194 (2010).

[22] J.-X. Cheng, A. Volkmer, L. D. Book, and X. S. Xie, J. Phys. Chem. B **106**, 8493 (2002).

[23] M. Müller and J. M. Schins, J. Phys. Chem. B **106**, 3715 (2002).

[24] T. W. Kee and M. T. Cicerone, Opt. Lett. **29**, 2701 (2004).

[25] A. Volkmer, J. Phys. D **38**, R59 (2005).

[26] B. von Vacano, L. Meyer, and M. Motzkus, J. Raman Spectrosc. **38**, 916 (2007).

[27] G. S. Agarwal, in *Quantum Optics*, edited by G. Höhler, Springer Tracts in Modern Physics Vol. 70 (Springer, Berlin, 1974), pp. 1–128.

[28] M. O. Scully and M. S. Zubairy, *Quantum Optics* (Cambridge University Press, Cambridge, 1997).

[29] M. Richter and S. Mukamel, Phys. Rev. A **83**, 063805 (2011).

[30] K. E. Dorfman, K. Bennett, Y. Zhang, and S. Mukamel, Phys. Rev. A **87**, 053826 (2013).

[31] S. Mukamel and S. Rahav, Adv. At. Mol. Opt. Phys. **59**, 223 (2010).

[32] A. Konar, J. D. Shah, V. V. Lozovoy, and M. Dantus, J. Phys. Chem. Lett. **3**, 1329 (2012).

[33] A. Konar, V. V. Lozovoy, and M. Dantus, J. Phys. Chem. Lett. **3**, 2458 (2012).

[34] G. Juzeliūnas and D. Andrews, in *Resonance Energy Transfer*, edited by D. L. Amdrews and A. A. Demidov (Wiley, New York, 1999), pp. 65–107.

[35] F. Schlawin, K. E. Dorfman, B. P. Fingerhut, and S. Mukamel, Phys. Rev. A **86**, 023851 (2012).

[36] F. Schlawin, K. E. Dorfman, B. P. Fingerhut, and S. Mukamel, Nature Communications **4**, 1782 (2013).

[37] F. C. Spano and H. Yamagata, J. Phys. Chem. B **115**, 5133 (2011).

[38] R. Lettow, Y. L. A. Rezus, A. Renn, G. Zumofen, E. Ikonen, S. Götzinger, and V. Sandoghdar, Phys. Rev. Lett. **104**, 123605 (2010).

[39] K. E. Dorfman and S. Mukamel, Phys. Rev. A **86**, 013810 (2012).

[40] Y. L. A. Rezus, S. G. Walt, R. Lettow, A. Renn, G. Zumofen, S. Götzinger, and V. Sandoghdar, Phys. Rev. Lett. **108**, 093601 (2012).